AD_____

Award Number: W81XWH-10-1-1017

TITLE: Chemically Modified Bacteriophage as a Streamlined Approach to Noninvasive Breast Cancer Imaging

PRINCIPAL INVESTIGATOR: Michelle E. Farkas, Ph.D.

CONTRACTING ORGANIZATION: University of California, Berkeley
                                             Berkeley, CA 94720
Á

REPORT DATE: October 201G
Á

TYPE OF REPORT: Annual Summary
Á

PREPARED FOR: U.S. Army Medical Research and Materiel Command
                 Fort Detrick, Maryland 21702-5012

DISTRIBUTION STATEMENT: Approved for Public Release;
                                     Distribution Unlimited

The views, opinions and/or findings contained in this report are those of the author(s) and should not be construed as an official Department of the Army position, policy or decision unless so designated by other documentation.

REPORT DOCUMENTATION PAGE

Form Approved
OMB No. 0704-0188

Public reporting burden for this collection of information is estimated to average 1 hour per response, including the time for reviewing instructions, searching existing data sources, gathering and maintaining the data needed, and completing and reviewing this collection of information. Send comments regarding this burden estimate or any other aspect of this collection of information, including suggestions for reducing this burden to Department of Defense, Washington Headquarters Services, Directorate for Information Operations and Reports (0704-0188), 1215 Jefferson Davis Highway, Suite 1204, Arlington, VA 22202-4302. Respondents should be aware that notwithstanding any other provision of law, no person shall be subject to any penalty for failing to comply with a collection of information if it does not display a currently valid OMB control number. **PLEASE DO NOT RETURN YOUR FORM TO THE ABOVE ADDRESS.**

1. REPORT DATE October 2012	**2. REPORT TYPE** Annual Summary	**3. DATES COVERED** 28 September 2011 – 27 September 2012

4. TITLE AND SUBTITLE

Chemically Modified Bacteriophage as a Streamlined Approach to Noninvasive Breast Cancer Imaging

5a. CONTRACT NUMBER

5b. GRANT NUMBER
W81XWH-10-1-1017

5c. PROGRAM ELEMENT NUMBER

6. AUTHOR(S)

Michelle E. Farkas, Ph.D.

E-Mail: mfarkas@berkeley.edu

5d. PROJECT NUMBER

5e. TASK NUMBER

5f. WORK UNIT NUMBER

7. PERFORMING ORGANIZATION NAME(S) AND ADDRESS(ES)

University of California, Berkeley
Berkeley, CA 94720

8. PERFORMING ORGANIZATION REPORT NUMBER

9. SPONSORING / MONITORING AGENCY NAME(S) AND ADDRESS(ES)
U.S. Army Medical Research and Materiel Command
Fort Detrick, Maryland 21702-5012

10. SPONSOR/MONITOR'S ACRONYM(S)

11. SPONSOR/MONITOR'S REPORT NUMBER(S)

12. DISTRIBUTION / AVAILABILITY STATEMENT
Approved for Public Release; Distribution Unlimited

13. SUPPLEMENTARY NOTES

14. ABSTRACT

By using efficient synthetic protocols to conjugate small molecules to phage coat proteins, we can directly convert cell surface marker specific phage isolated from library screens into imaging agents that can target and differentiate breast cancer tissues. In the current work, I have utilized phage evolved to target HER3, CD44, and CD73 cell surface proteins, in addition to those previously described that bind EGFR and HER2. The abilities of the modified phage to bind their targeted cell surface receptors following chemical manipulations were evaluated in vitro by using flow cytometry and confocal microscopy assays, and it was found that the synthetic modifications performed did not significantly alter phage binding ability. Experiments in vivo with mouse xenograft models were used to determine biodistribution and tumor targeting abilities of the agents in a physiological setting. Follow-up experiments using radio-tracers for thorough evaluation of bio-distribution and stability are currently in progress. Phage were also explored as agents for immunofluorescence staining of breast cancer tissues as a surrogate for tumor binding.

15. SUBJECT TERMS
Bacteriophage, cancer imaging, bio-distribution, cellular targeting

16. SECURITY CLASSIFICATION OF:			**17. LIMITATION OF ABSTRACT**	**18. NUMBER OF PAGES**	**19a. NAME OF RESPONSIBLE PERSON**
a. REPORT	**b. ABSTRACT**	**c. THIS PAGE**			USAMRMC
U	U	U	UU	52	**19b. TELEPHONE NUMBER** *(include area code)*

Table of Contents

INTRODUCTION: Diagnostic imaging methods, such as positron emission tomography (PET), play a key role in the detection, treatment, and study of breast cancer. Yet while enabling disease visualization, current imaging methods yield little information with regard to the type of cancer present, and biopsy follow-ups are required to determine patient prognoses and recommended treatment regimen. As a non-invasive alternative, my research involves the chemical modification and subsequent use of filamentous bacteriophage targeting specific breast cancer markers in order to visualize and study these cells and tumors in culture, immunohistology, and mice. The generation of imaging agents relies on the attachment of functional groups that can be detected (e.g. radioactive or fluorescent labels) to a molecule that shows some specificity for a marker of interest on the cell surface. The binding moieties are selected through the use of phage display techniques where members of a library of diversified phage are isolated based on their ability to associate with a particular target. We have demonstrated that we can selectively modify significant quantities of the pVIII coat proteins lining the sides of the phage in order to incorporate these labels and other small molecules. Following generation and modification of the targeted agents, their selectivity is evaluated *in vitro* and *in vivo*. By directly converting phage recovered from library screens into imaging agents, this research has the potential to significantly stream-line the process of targeted imaging agent generation.

BODY: My research involves the use of chemically modified filamentous (fd) bacteriophage in the targeting and differentiation of breast cancer tissues bearing specific surface markers, directly converting library-identified phage into imaging agents. In the first year of the fellowship, I generated and modified HER2 and EGFR-targeting phage to display small molecules, and performed *in vitro* evaluations of the phage's abilities to bind breast cancer and other cell lines that express the targeted markers of interest at varying levels. Xenograft models of breast cancer have been prepared in order to perform preliminary optical imaging experiments to evaluate phage tumor targeting capabilities. In the second year of the fellowship, I have expanded the repertoire of cell surface markers targeted to include CD44, HER3, and CD73. Using methods established earlier in this project, phage targeting these markers were modified and evaluated *in vitro* and *in vivo*. Means of cellular uptake and subsequent effects of endocytosis on phage have also been explored. Panels of phage will be used in histology experiments in the near future, using cell buttons derived from cell lines of interest as tumor surrogates. Based on our lack of positive findings using *in vivo* optical imaging, further efforts are currently being invested in radiolabeling of the agents (fluorophore quenching may play a significant role) and subsequent stability and bio-distribution evaluations, and preliminary *in vivo* evaluation of the MS2 icosahedral bacteriophage scaffold described below and in my project narrative.

Task 1. Generation and *in-vitro* evaluation of PET imaging agents based on filamentous phage. Based on moieties displayed on their terminal pIII capsid proteins, other groups have previously demonstrated the localization of phage *in vivo* to the prostate and prostate carcinoma,[1,2] and other targets.[3,4] In our research, we use filamentous bacteriophage (fd) that display marker-specific single-chain variable fragment (scFv) molecules identified by our collaborators in the laboratory of James D. Marks, M.D., Ph.D. (UCSF) using molecular evolution techniques. In studies described in the previous annual report, I used fd that are selective for the epidermal growth factor receptor (EGFR)[5] and human epidermal growth factor receptor 2 (HER2 or ERBB-2),[6] while phage targeting botulinum toxin serotype A (BoNT/A)[7] were used as a control. In the current work, phage targeting HER3, CD44, and CD73 have been generated and modified for evaluation *in vitro* and *in vivo*. The overexpression of HER3 has been shown to be a marker of reduced patient breast cancer-specific survival.[8] CD44 is a cell adhesion molecule involved in tumor metastasis and a marker used to identify human cancer stem cells,[9,10] while CD73 is a cell surface protein overexpressed in many solid tumors that may promote tumor progression.[11,12]

    Escherichia coli (*E. coli*) infected with anti-HER3, -CD44, and -CD73 phage had been generated by the Marks group and given to the Francis lab in order further propagate fd of interest for our studies, along with methodology to do so.[13] I had previously optimized a number of the steps required for phage production but found that recovery continued to be dependent upon phage type and time since re-plating of *E. coli* colonies. Phage targeting EGFR, HER2, HER3, CD44, and CD73 were each produced several times for further modification and experiments. The optimized procedure for phage production is described in the *methods* section of this report and ***Appendix 1***: Reprint of ACS Nano Journal Article (including Supporting

Information).[14] An overview of the chemical modification strategy used for subsequent phage modification is shown in **Figure 1**. The conditions used for the transamination and appendage of small molecules via oxime formation following the production of phage proteins are reiterated from the previous annual report in the *methods* section and also described in *Appendix 1*. Similar protocols were used for both new and previously described phage. *In vivo* biodistribution experiments with anti-HER3, -CD44, and -CD73 phage are described later in this report.
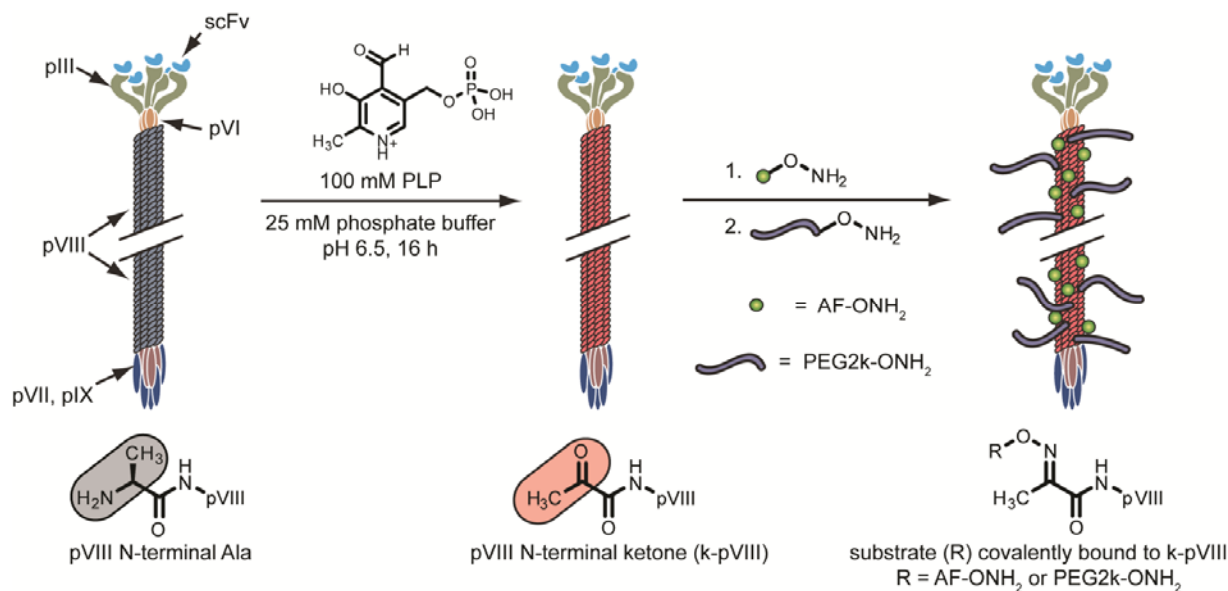
Figure 1. Chemical modification of filamentous (fd) phage. N-terminal alanines (Ala) of the pVIII coat proteins lining the filamentous phage are converted to ketone groups that can be subsequently modified with small molecule alkoxyamines, including dyes (AF-ONH$_2$) and polyethylene glycol chains (PEG2k-ONH$_2$).

As these agents are intended for imaging use *in vivo*, I sought to enhance the characteristics of the phage by appending polyethylene glycol (PEG) chains, which have been shown to increase the plasma circulation times of proteins, liposomes, and other nanoparticles via shielding and other effects.[15-17] Our previous work demonstrated that various numbers of PEG chains (molecular weight 2,000 Da, PEG2k) could be introduced per phage, ranging from 20-70% modification of coat proteins or 900-3150 copies per phage, as determined by reverse-phase HPLC, while zeta potential measurements showed that increased numbers of 2 kDa PEG chains shield surface charge.[14] In the previous annual report, PEG-AF-647-anti-EGFR phage were generated with varying levels of PEG (10%, 25%, 50%, and 75%), and evaluated with regard to cell binding and *in vivo*.

At the time of proposal submission, preliminary studies involving the labeling of fd with ^{18}F had been performed via the oxidative coupling of ^{18}F-fluoroaniline to small molecule alkoxyamines containing aminophenol groups. However, the reaction times required to generate the desired radio-labeled phage products proved to be incompatible with the short-lived ^{18}F isotope, whose half-life is 109 minutes, and labeling of PEGylated phage was minimal. Concurrently, in order to thoroughly evaluate the circulation, stability, and clearance properties of these agents, a longer-lived radionuclide was deemed to be required. For these reasons, we have begun to explore the use of ^{64}Cu, whose half-life is 12.7 hours, which we envision to be incorporated via chelation to 1,4,7,10-tetraazacyclododecane-1,4,7,10-tetraacetic acid (DOTA) or 1,4,7-triazacyclononane-*N*,*N*',*N*''-triacetic acid (NOTA) that would be appended to the phage in an earlier step. Chemical methodologies for the modification of phage with ^{18}F are still being sought.

The biomarker binding site at the phage terminus is presumed to be located a few nanometers from the bulk of the chemical modifications, thereby minimizing interference with scFv binding (**Figure 1**). In previous work testing the potential for interference, anti-EGFR fd were minimally functionalized with AF-488 fluorescent dye molecules and varying numbers of 2 kDa PEG chains. Using flow cytometry, these samples were evaluated for their ability to bind MDA-MB-231 cells (EGFR-positive) and compared to control phage (anti-BoNT/A), which do not bind EGFR. Excellent binding selectivity was observed at all levels of PEG

modification, although increased levels of PEG resulted in slightly diminished binding. Neither anti-EGFR nor anti-BoNT/A phage bound to SUM-52PE cells, which lack EGFR.[14] Following reactions yielding increased levels of AF-488 modification, anti-EGFR, anti-HER2, and anti-BoNT/A phage binding were evaluated via flow cytometry in a panel of receptor positive and negative cell lines, including both basal and luminal sub-type immortalized breast cancer cells of a variety of origins. These data have been described in the previous annual report.

Newly described phage targeting CD44, HER3, and CD73 receptors have been similarly modified with AF488 or AF647 fluorophores, and their selectivity for breast cancer cell line binding were evaluated. Representative data from flow cytometry experiments in MDA-MB-231 (basal, adenocarcinoma), MCF-7 clone 18 (a HER2-overexpressing variant of the luminal, adenocarcinoma cell line MCF-7), HCC1954 (basal, ductal carcinoma), and MDA-MB-468 (basal, adenocarcinoma) are shown in **Figure 2**. The procedures used are described in the *methods* section and are similar to those in the previous annual report and in ***Appendix 1***; forward- and side-scatter plots are included in the *supporting information* section at the conclusion of this report. Cell-based flow cytometry analyses were subsequently used as 'quality-control' in order to assess the abilities of phage to bind targeted cells following various chemical modifications and reaction optimizations, and prior to use in any other assays.
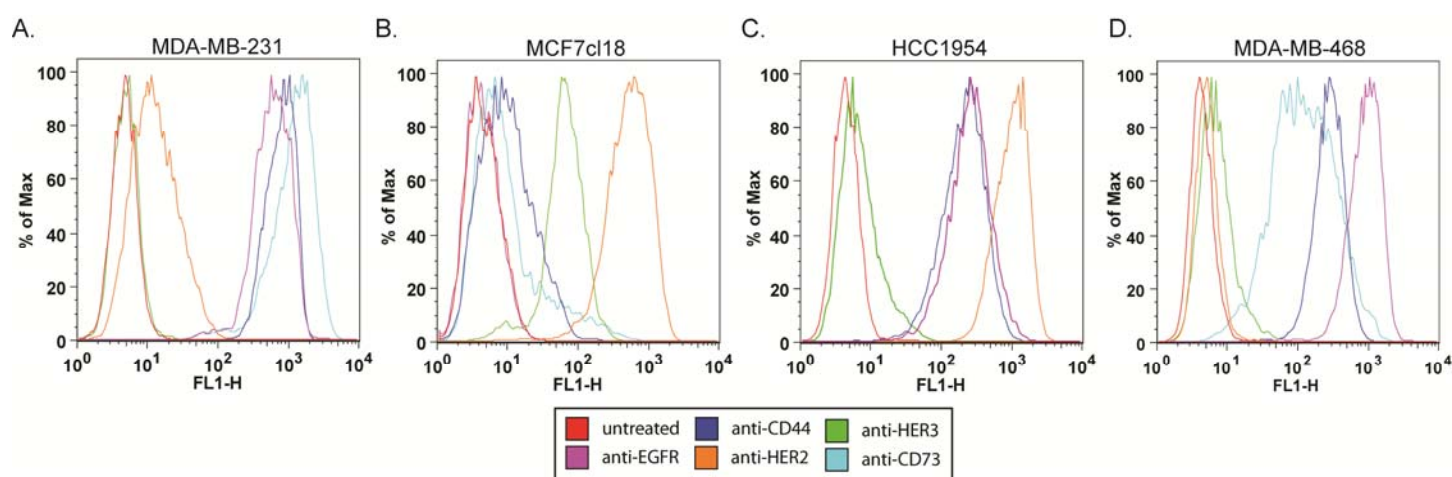
Figure 2. Representative flow cytometry data from phage binding experiments. Histograms are shown for (**A**) MDA-MB-231, (**B**) MCF-7 clone 18, (**C**) HCC1954, and (**D**) MDA-MB-468 cells (see description below) treated with anti-EGFR (purple), anti-HER2 (orange), anti-CD44 (navy), anti-HER3 (green), and anti-CD73 (light blue) phage. Untreated cells are shown in red. Forward- and side-scatter data for these plots are shown in *supporting information*.

In the previous annual report, a live-cell confocal microscopy protocol was devised in order to visualize phage cell binding and uptake.[14] Experiments were performed using the breast cancer cell lines HCC1954, MDA-MB-231, and MCF-7 clone 18. Anti-EGFR and anti-HER2 phage were labeled with AF-488 and AF-647, respectively. MDA-MB-231 and MCF-7 clone 18 cells were both individually treated with each type of phage and co-cultured and treated with both types of phage concurrently, while HCC1954 cells, which overexpress both HER2 and EGFR, were both separately and simultaneously treated with each phage type. In addition to obtaining confocal microscopy images with anti-CD44 (**Figure 3**), -HER3, and -CD73 phage types using these cell lines, we have included the use of MDA-MB-468 cells, since they possess no detectable levels of HER2.[18] The procedures used are described in the *methods* section and are similar to those in the previous annual report and in ***Appendix 1.***
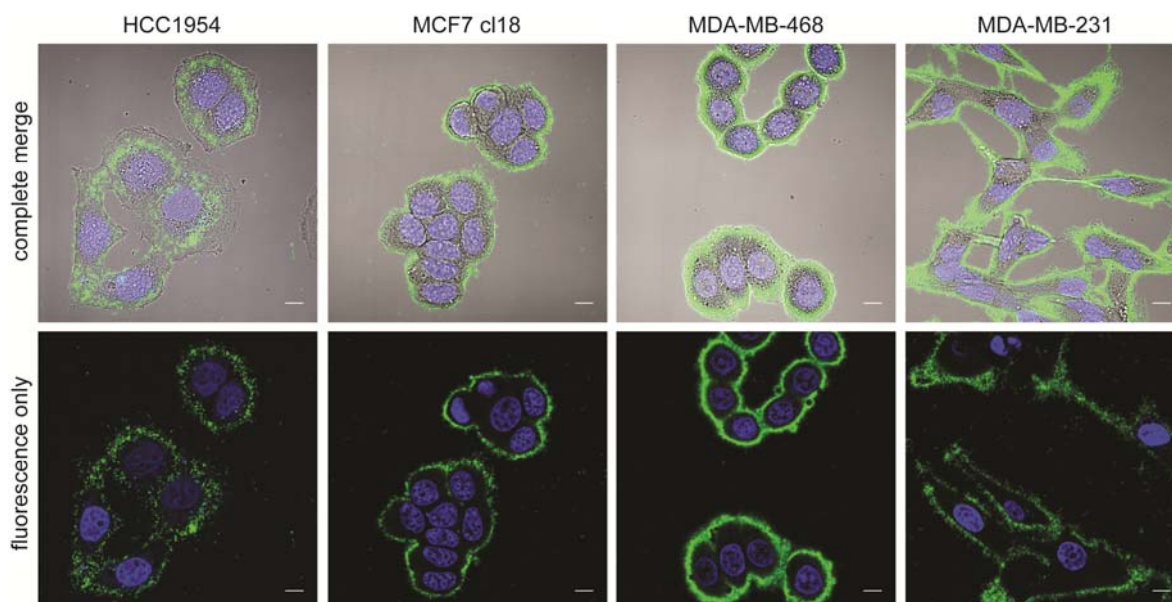
**Figure 3. Live-cell confocal microscopy of anti-CD44 phage**. CD44-targeted phage (green) binding to HCC1954, MCF-7 clone 18, MDA-MB-468, and MDA-MB-231 cells is shown. Nuclei have been stained with DAPI (blue). Both the complete merge (top row), and fluorescence-only (bottom row) images are shown. Scale bars indicate 10 μm.

At the time of the writing of the previous annual report, it was noted that following prolonged phage exposure to cells, uptake was observed in several instances. Further microscopy experiments to evaluate cellular uptake of phage and the mechanism by which it occurs have since been conducted. By postponing imaging for a short period of time (<1 hr) following phage incubation with cells of interest, striking differences in the accumulation of phage within cells have been noted with and without the dynamin inhibitor dynasore[19] (**Figure 4**). Dynasore is a cell-permeable small molecule that inhibits the GTPase activity of dynamin, essential for clathrin-dependent coated-vesicle formation. Protocols used in the assay are described in the *methods* section.
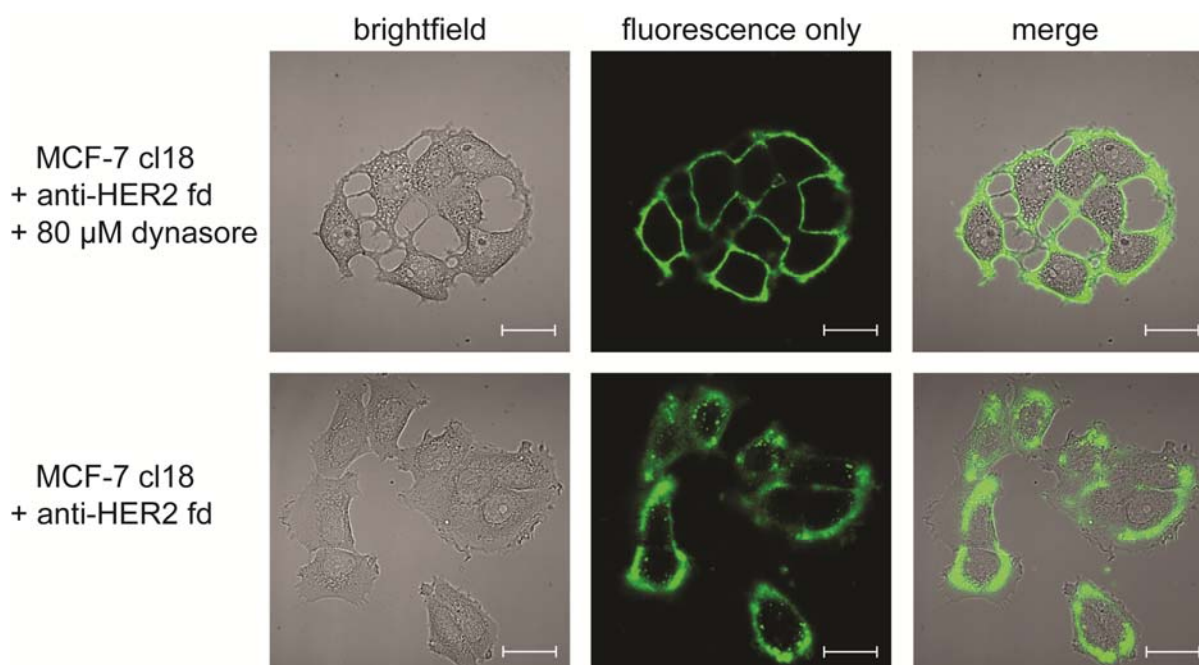
Figure 4. Live cell imaging of phage endocytosis disruption. Anti-HER2 phage (green) binding to MCF-7 clone 18 cells is shown. (Top row) Cells treated with dynasore are unable to undergo dynamin-dependent endocytosis and phage remain localized to the cell membrane. (Bottom row) Cells not treated with the small molecule display phage located within the cell interior. Scale bar = 20 μm.
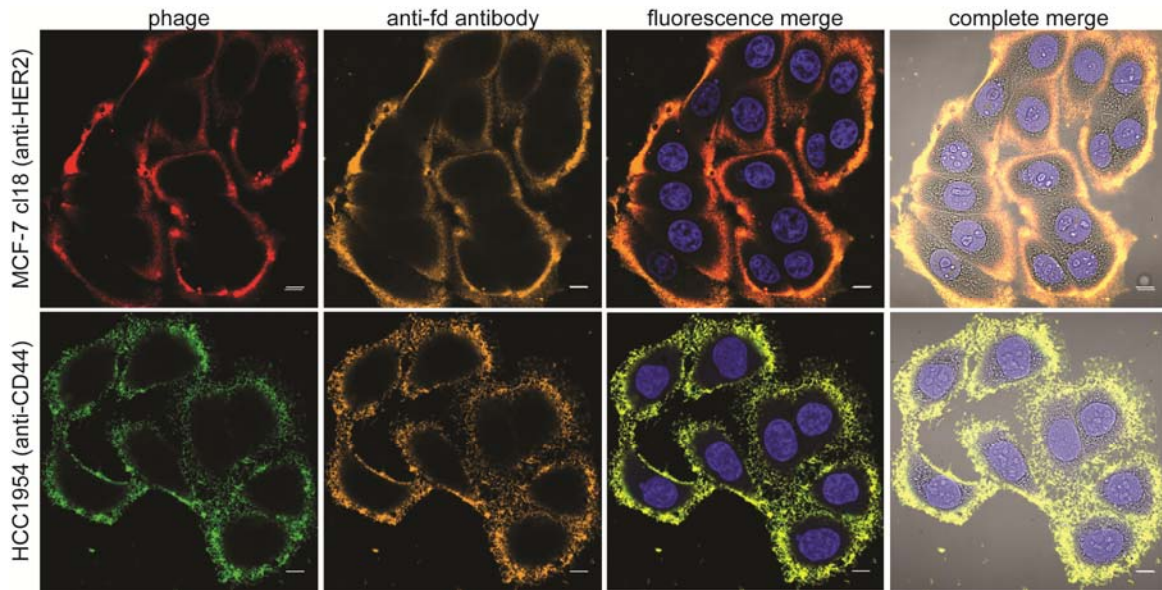
Figure 5. Evaluation of phage fate following endocytosis. Anti-HER2 phage (red) and anti-CD44 phage (green) binding to MCF-7 clone 18 cells (top row) and HCC1954 cells (bottom row), respectively, are shown. Following incubation of cells with phage, cells were fixed and permeabilized to allow anti-fd antibodies (orange) to bind to phage. Co-localization of antibodies and phage reveals that phage remain intact following endocytosis. Cell nuclei are stained with DAPI (blue). Scale bar = 10 μm.

Following observation of phage uptake by cells via clathrin-mediated endocytosis, we wanted to ensure that the phage remained intact following internalization. In order to obtain confirmation, antibodies targeting fd (anti-fd) were used to assess whether the phage structures had undergone degradation or remained stable (**Figure 5**). If the entire phage protein was not present, the antibody would not bind. Cell lines of interest were treated with phage; following incubation, unbound phage was washed away and cells were fixed and permeabilized to allow the antibodies to pass through the cell membrane. Both fluorescent secondary antibody and fluorescent anti-fd were used for visualization; both gave similar results. Based on analysis using confocal microscopy, phage and anti-fd co-localized, and the agents were presumed to remain intact. Protocols used in the assay are described in the *methods* section.

Based on the lack of tumor uptake of phage previously observed and described *in vivo*, we planned to add means by which we could assess tumor binding *in vitro*. By using cell buttons, which are parafin-embedded sections of tumors that can be mounted on slides for visualization using microscopy, we can use cell lines identical to those used in xenograft tumor models for additional phage binding experiments. These entities are intended to mimic the tumors by possessing similar cell distribution and association characteristics, which are neither present in the mixtures of suspended cells used for flow cytometry nor cultured adhered cells used for confocal microscopy experiments. Since the phage used were identified based on their abilities to bind to live cells, prior to utilization of the cell button constructs, binding experiments using fixed cells were conducted (**Figure 6**). Experiments using mounted cell button slices as tumor surrogates to evaluate binding of phage are currently underway.
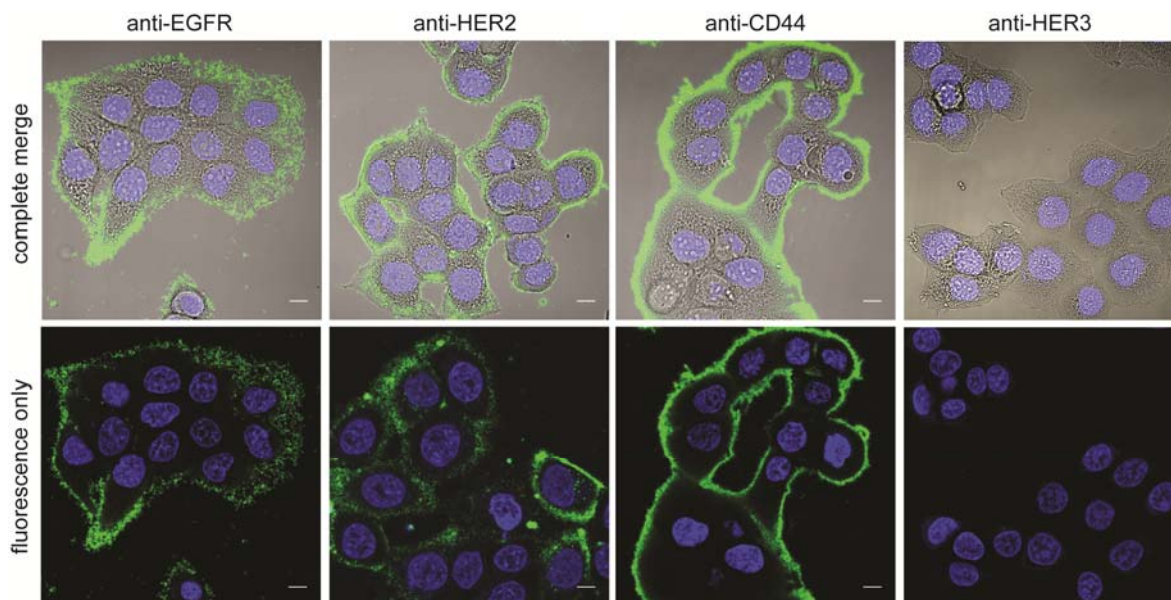
Figure 6. Evaluation of phage binding to fixed HCC1954 cells. Anti-HER2, -EGFR, -CD44, and –HER3 phage (green) binding to fixed cells was determined. As an example, HCC1954 cells are shown. Complete merge (top row), and fluorescence only (bottom row) images are shown. Nuclei are stained with DAPI (blue). Scale bar = 10 μm.

Experiments to detect non-specific phage binding in serum (rat, rabbit, or mouse), as described in the statement of work and mentioned in the previous annual report have not yet been conducted. We are currently developing HPLC methods using size exclusion chromatography (SEC) in order to be able to quantify phage stability in blood/serum and radiochemical purity following labeling. Upon determining successful conditions, we plan to concurrently evaluate phage stability and non-specific binding in a series of experiments.

Task 2. *In vivo* animal imaging with ^{18}F agents. In the previous annual report, the evaluation of phage bio-distribution in healthy animals had been postponed pending the completion of initial optical imaging experiments using tumor bearing mice and optimization of the chemistry to modify the agents with ^{18}F. As mentioned above, it was deemed that the suitability of ^{18}F and the reaction conditions used for its incorporation for evaluation of phage biodistribution and tumor targeting experiments were non-ideal. For this reason, we are exploring the use of ^{64}Cu and its chelation using DOTA and/or NOTA. In combination with the aforementioned HPLC method development for determination of radiochemical purity, we anticipate that this system will provide a comprehensive assessment of phage circulation and fate.

Initial animal experiments had been carried out prior to submission of the previous annual report. These studies used fluorophore labeled anti-EGFR, anti-HER2, and anti-BoNT/A phage with a fluorescence molecular tomography optical imaging system. We chose to use optical imaging because results from *in vitro* cell culture binding experiments could be directly correlated with *in vivo* targeting, as identical agents are used for both assays. Two distinct experiments were performed: in one, mice with xenografted HCC1954 cells in the hind flank were imaged with AF-647 modified HER2-targeting phage, while in the other, mice orthotopically implanted with MDA-MB-231 cells in the mammary fat pads were imaged with anti-EGFR and anti-BoNT/A phage. The agents did not appear to be taken up by the tumor, and possessed similar localization profiles independent of targeting group. Major sites where the phage accumulated included the liver and kidneys, followed by the bladder. In both cases, phage also appeared to localize in the area of the tumor/inguinal lymph nodes. The majority of the agents were found to clear after 48-72 h.

In the current period of time, I have used phage targeting HER2, HER3, CD44, and CD73 labeled with AF-647 to image mice that have been orthotopically implanted with MCF-7 clone 18 and MDA-MB-231 cells on opposite mammary fat pads. In the prior annual report, xenografts generated using HCC1954 cells exhibited problems including growth of and consistency within (including potential presence of cysts) the tumors. By using MCF-7 clone 18 and MDA-MB-231 cells concurrently, we are able to generate models that possess

internal controls where an agent targets markers present in one cell line but not another. One of the issues requiring attention in the use of two separate cell lines in xenografts is the synchronization of tumor size. In this case, the tumors derived from MCF-7 clone 18 cells (right side) grew more quickly than those from MDA-MB-231 cells (left side). Shown are representative results from imaging with anti-HER2 (**Figure 7**) and anti-CD44 phage (**Figure 8**). All agents were injected via the tail vein and imaged at the following time points: pre-injection, 10 min, 30 min, 1 h, 2 h, 3 h, 4 h, 5 h, 6 h, 7 h, 8 h, 24 h, 48 h, 72 h. Following imaging at the final time point, animals were sacrificed, and *ex-vivo* bio-distribution was performed (data not shown). Unfortunately, all agents examined appeared to behave similarly to each other and to those from previous experiments. Major sites where the phage accumulated included the liver and kidneys, followed by the bladder. Additional sites of accumulation determined from *ex-vivo* biodistribution included the spleen, pancreas, and lungs. Small amounts were found in the tumors. Experimental details can be found in the *methods* section.
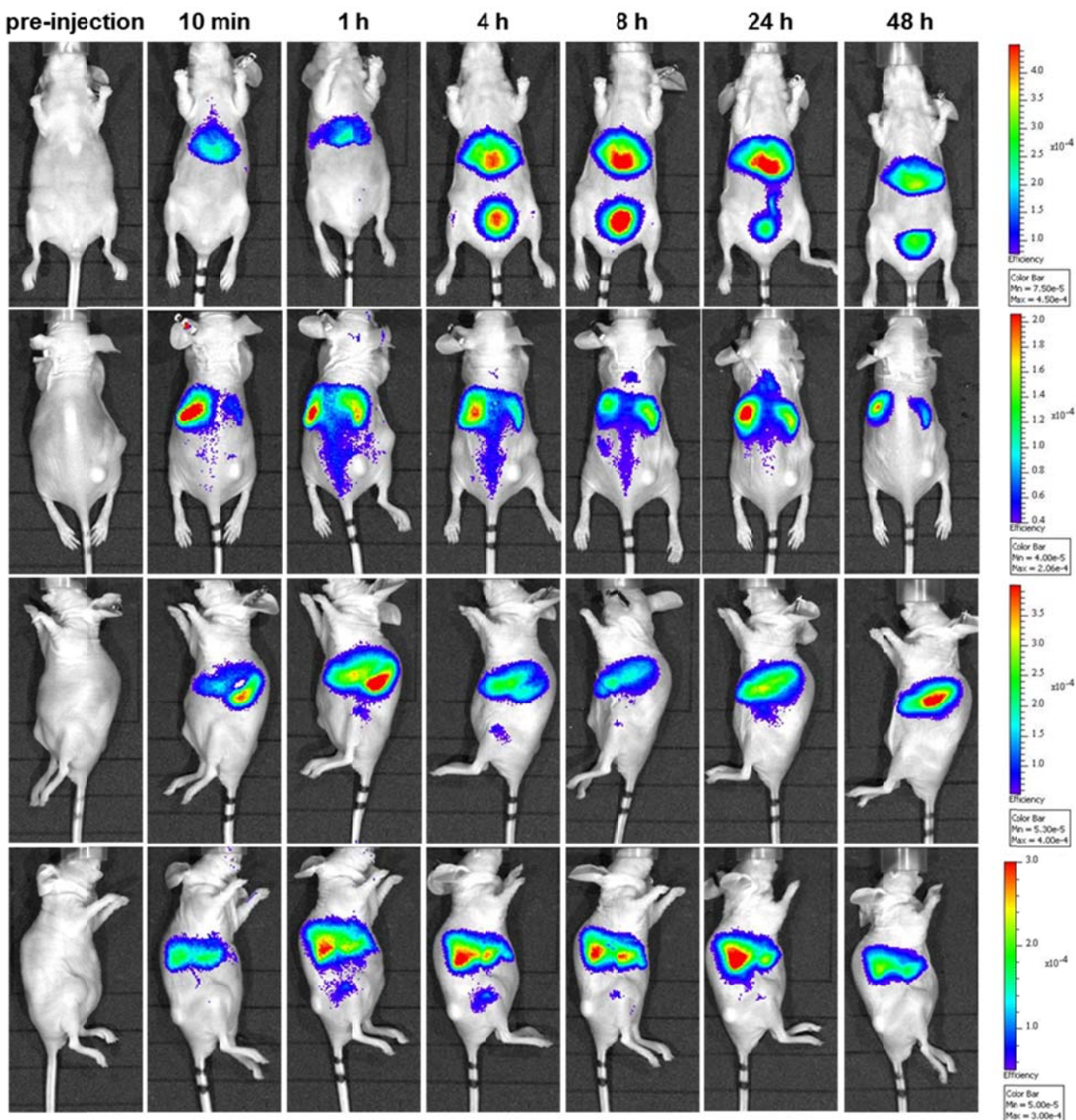
Figure 7. Imaging of mice implanted with MCF-7 clone 18 and MDA-MB-231 human breast cancer cells with anti-HER2 phage. Representative images for mice injected with anti-HER2 phage via the tail vein in the supine, prone, and side positions over the course of 48 h. In the supine images, the agent is primarily observed in the liver and bladder, while in the prone position, the kidneys are also observed. All images were acquired from a single mouse injected with anti-HER2 phage, and normalized to the same scale.
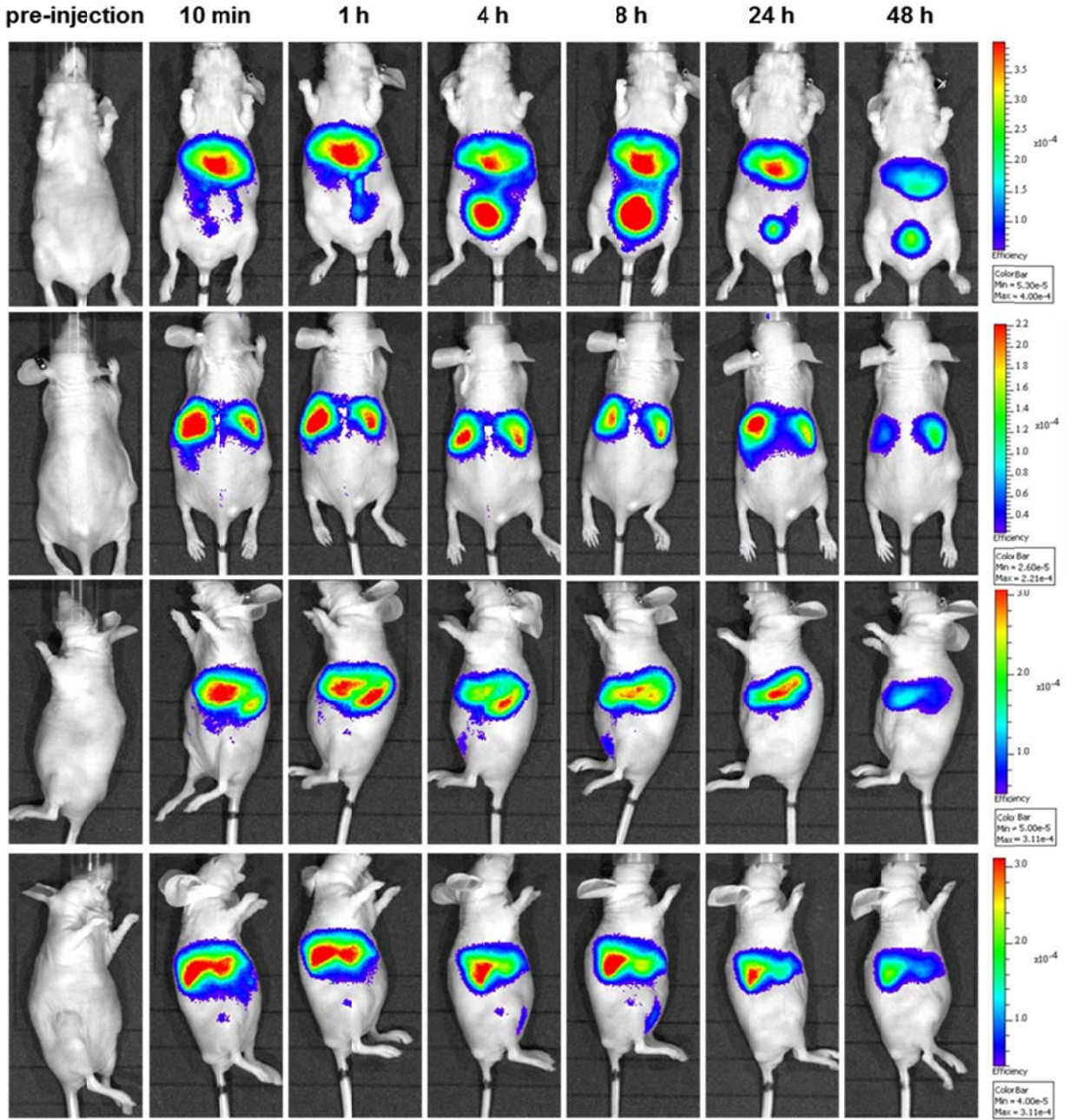
Figure 8. Imaging of mice implanted with MCF-7 clone 18 and MDA-MB-231 human breast cancer cells with anti-CD44. Representative images for mice injected with anti-CD44 phage via the tail vein in the supine, prone, and side positions over the course of 48 h. In the supine images, the agent is primarily observed in the liver and bladder, while in the prone position, the kidneys are also observed. All images were acquired from a single mouse injected with anti-HER2 phage, and normalized to the same scale.

One of the means by which we had initially planned to improve agent circulation and bio-distribution properties was the appendage of PEG chains (PEG2k), as described above. Phage were previously modified with PEG2k and found to bind to their targeted cell surface markers *in vitro*. The PEG likely improved circulation as visualized via optical imaging (where the amount of time taken for maximum amounts of signal to reach the liver were 1 h for 0% P8 modification with PEG2k, and 3 h for 25% P8 modification with PEG2k). However, optical imaging experiments were found to be generally inconclusive for the following reason: despite the acknowledged presence of fluorophore quenching present on the phage, we cannot determine the magnitude of signal increase potentially occurring as the result of fluorophore liberation following phage

11

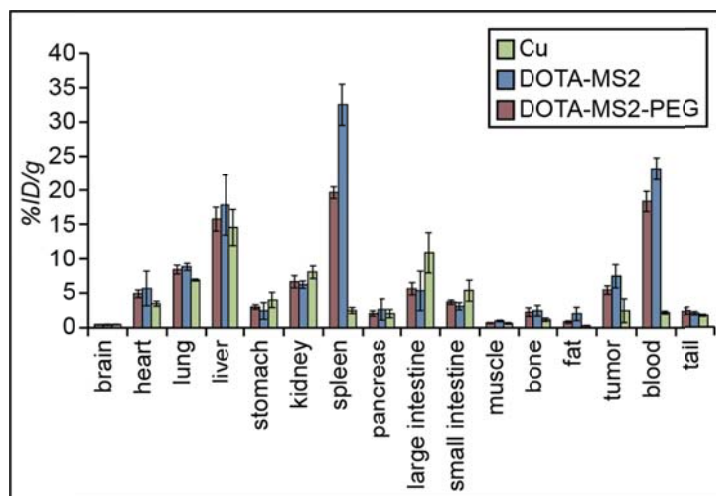degradation in the liver/hepatic system. For this reason, we are concurrently exploring means of labeling phage with radionuclides, as they will not exhibit any quenching, and assessing the stability of the phage protein following *in vivo* studies, which will have passed through the hepatic system.

Following the inconclusive *in vivo* results obtained from experiments using filamentous phage, initial studies using the icosahedral bacteriophage MS2, described in the research proposal as an alternative phage-based imaging system, have been undertaken. Since the previous annual report, other members of the Francis group have developed protocols for the labeling of these viral capsids with ^{64}Cu, while methods to append PEG to the exterior of the capsids have been previously described.[20] Using these procedures, PET studies using ^{64}Cu-labeled MS2 (**Figure 9a**) and MS2-PEG (**Figure 9b**), and corresponding *ex vivo* analyses (**Figure 10, Table 1**) were performed to initially assess the bio-distribution properties of this scaffold prior to further investigation with any targeted moieties versus free ^{64}Cu (*supporting information*). Surprisingly, these agents remained in circulation even 24 h following injection. Further studies to characterize their bio-distribution properties are pending. Additional information regarding procedures for this study may be found in the *methods* section.
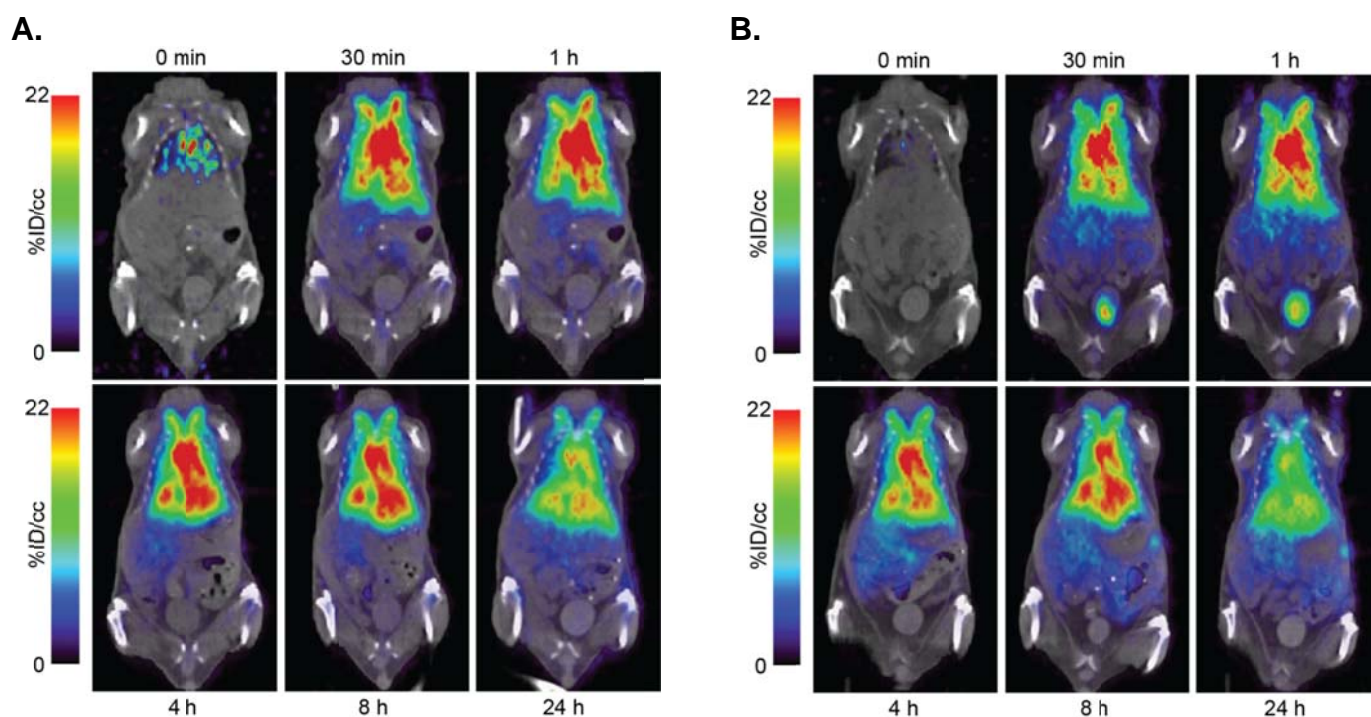
Figure 9. PET imaging of mice with MS2 viral capsids. PET-CT images from a mouse imaged with (**A**) ^{64}Cu-labeled MS2 and (**B**) ^{64}Cu-labeled PEG-MS2. A dynamic scan was performed over the first 60 min, followed by scans obtained at 4, 8, and 24 h. All images have been decay-corrected and normalized. The scales are reported as percent injected dose per milliliter (%ID/cc).

Figure 10 . Biodistribution of MS2 viral capsids in mouse organs. Organ-based bio-distribution of free [64]Cu (used as control), ^{64}Cu-labeled MS2, and ^{64}Cu-labeled PEG-MS2, as determined by gamma-counting. Organs were weighed following excision, and decay corrections were calculated for each sample based on individual agent standards. Each agent was administered to 3 animals. The height of each bar represents the average percentage of the injected dose per gram (%ID/g). Error bars indicate the standard deviation of the samples.

Table 1. Biodistribution of ^{64}Cu-labeled agents in mice.[a]

Organ	[64]Cu only	MS2	MS2-PEG
brain	0.5 ± 0.1	0.4 ± 0.0	0.4 ± 0.0
heart	3.5 ± 0.4	5.7 ± 2.5	4.9 ± 0.5
lung	6.9 ± 0.1	8.8 ± 0.5	8.4 ± 0.6
liver	14.5 ± 2.6	17.8 ± 4.4	15.8 ± 1.7
stomach	4.0 ± 1.1	2.4 ± 1.2	3.0 ± 0.3
kidney	8.1 ± 0.9	6.3 ± 0.5	6.7 ± 0.9
spleen	2.5 ± 0.4	32.5 ± 3.0	19.6 ± 0.8
pancreas	2.0 ± 0.6	2.6 ± 1.5	2.0 ± 0.4
large intestine	10.9 ± 2.9	5.4 ± 2.9	5.6 ± 0.9
small intestine	5.4 ± 1.5	3.1 ± 0.5	3.7 ± 0.3
muscle	0.6 ± 0.1	1.0 ± 0.1	0.7 ± 0.1
bone	1.2 ± 0.2	2.4 ± 0.8	2.2 ± 0.6
fat	0.3 ± 0.0	2.0 ± 1.0	0.8 ± 0.2
tumor	2.4 ± 1.7	7.5 ± 1.7	5.4 ± 0.6
blood	2.2 ± 0.2	23.1 ± 1.6	18.3 ± 1.5
tail	1.7 ± 0.1	2.0 ± 0.2	2.3 ± 0.5

[a]Numbers are reported as the average of the percent injected dose per gram of tissue (%ID/g), plus or minus the standard deviation observed across three subjects.

Methods:

1. <u>Phage propagation from infected *E. coli.*</u> All phage described herein were generated and purified using identical conditions. A single colony of *E. coli* TG1 cells infected with fd phage are inoculated into 5 mL of LB media containing 15 μg/mL tetracycline (a tetracycline-resistance gene was previously introduced into the genome), followed by incubation with shaking at 37 °C and 250 rpm. After approximately 9 h of growth, the starter culture was split in half -- 2.5 mL of the culture was added to 1 L of 2xYT media. The culture was incubated at 30 °C for 16-18 h at 250 rpm. The media was recombined and the cells were removed via centrifugation at 6,000 rpm for 20 min at 4 °C. The supernatant was collected and fd phage were precipitated for 1 h at 4 °C (on ice) after addition of and thorough mixing with 1/10 volumes of 20% PEG8k/2.5M NaCl solution (200 mL for 2 L media). The resulting suspension was centrifuged at 8,000 rpm for 30 min at 4 °C, and the recovered pellet(s) were resuspended in a total volume of 35 mL PBS. The resulting phage solution was centrifuged at 6,000 rpm for 20 min at 4 °C to remove additional cellular debris. The supernatant was collected, and fd were precipitated for 1 h at 4 °C (on ice) after addition of and thorough mixing with 1/10 volume 20% PEG8k/2.5M NaCl solution. The samples were centrifuged at 9,000 rpm for 30 min at 4 °C to isolate the phage. The resulting pellet was resuspended in 3-9 mL of 4 °C PBS and stored at 4 °C.

2. <u>PLP-mediated transamination.</u> Fd phage were transaminated using 100 mM PLP in 100 mM phosphate buffer at r.t., pH 6.5 for ~16 h. As a result of the large excess of PLP used, phage concentrations were not found to be critical, but were typically 25-150 nM. In order to prepare the PLP solution, a sufficient volume of 250 mM phosphate buffer, pH 6.5 is added to solid PLP to make a 2 M solution (0.53 g in 1 mL). The pH is adjusted to 6.5 using 3 M NaOH (~0.5 mL), and 250 mM phosphate buffer, pH 6.5 is added to give a 1 M PLP solution. This solution must be made freshly before each use – do not freeze or store. The total reaction volume is 10 mL: 3 mL phage, 5 mL NANOpure water, 1 mL 250 mM phosphate buffer, pH 6.5, and 1 mL 1 M PLP solution generated as above. The reaction is allowed to proceed for 16-18 h at r.t. The phage are precipitated for 1 h at 4 °C after thorough mixing with 1 mL (1/10 volume) 20% PEG8k and 2.5 M NaCl, followed by centrifugation at 8,000 rpm for 30 min. The pellet is resuspended in 10 mL PBS, and the precipitation and centrifugation steps

repeated. The pellet is then resuspended in 1 mL PBS, concentration determined by UV-vis, and precipitated and centrifuged; a final resuspension in PBS is performed to bring phage concentration to 250-400 nM. Phage are stored at 4 °C.

3. <u>Fluorophore labeling.</u> Modification of the phage with AF-488 dye is performed using the following reagent concentrations: 185 nM phage, 20 mM phosphate buffer, pH 6.2, 10 mM aniline, and 1 mM AF-488-ONH$_2$, PBS (to bring the reaction mixture to the correct volume; reactions are typically carried out on a 50 or 100 μL scale). The phage, phosphate buffer, and PBS are added and mixed thoroughly. The dye is then added, followed by aniline, with thorough mixing accompanied by each addition. The reaction is allowed to proceed in the dark at r.t. for 16-18 h. Following reaction, the solution is diluted to 1 mL, and the same method for precipitation and centrifugation is used as in the PLP modification. Phage are precipitated/centrifuged/re-suspended twice; the final re-suspension is in a volume of PBS to give ~200 – 300 nM phage. Phage concentrations and levels of fluorophore modification are determined by UV-vis. For higher levels of phage modification and modification using AF-647, all steps are identical; however, 100 mM (neat) aniline is used as opposed to 10 mM.

4. <u>Flow cytometry binding assay.</u> All cells were maintained using ATCC recommended guidelines. Cells were washed with PBS, trypsinized, and following quench with FBS-containing media, harvested from T75 or T175 flasks. Cells were centrifuged at 125 rcf for 5 min, and resuspended in media. Following counting via hemocytometer, the cells were centrifuged again, and resuspended in cold flow cytometry buffer (1% FBS in DPBS) at 5 million cells/mL. The cells were aliquotted into eppendorf tubes at 100 μL (500,000 cells) per tube and kept on ice. 100 μL of 0.8 nM phage in flow cytometry buffer is added to each sample (100 μL PBS is added to 'untreated' samples), and are incubated for 1 h on ice in the dark. After 1 h, each sample is diluted to 1 mL with flow cytometry buffer, and the tubes are centrifuged at 2000 rpm for 5 min. The supernatant is removed, and cells are resuspended in 1 mL flow cytometry buffer, followed by centrifugation, and removal of the supernatant. The cells are finally resuspended in 200 μL flow cytometery buffer, and transferred to flow cytometry tubes. Flow cytometry experiments were performed on a FACSCalibur flow cytometer (BD Biosciences, USA) equipped with 448 nm and 633 nm lasers.

5. <u>Confocal microscopy imaging.</u> All cells were maintained using ATCC recommended guidelines. Cells were harvested as above. Following counting via hemocytometer, cells were resuspended in normal growth media at a concentration of 25,000 cells/mL; 2 mL was added to each 35 mm glass bottom dish (MatTek Corp.). For MCF-7 clone 18/MDA-MB-231 co-cultures, 1 mL (25,000 cells/mL) of each cell line was added to a centrifuge tube and mixed by pipetting prior to plating in dishes together. Cells were allowed to grow at 37 °C with 5% CO$_2$ for 72-96 h. All media was removed from the dishes, and cells were washed once with 1 mL PBS. 150 μL of 0.8 nM phage in flow cytometry buffer (see above) was added to each well of the plate, and the dishes were returned to an incubator at 37 °C with 5% CO$_2$. After 1 h, 1 mL room temperature flow cytometry buffer was added to gently wash the cells and removed; 2 more washes with 1 mL r.t. flow cytometry buffer were performed, and then 1 mL phenol red-free media (with FBS) was added to the cells. DAPI was added at 1 μM prior to imaging. Images were acquired on a Zeiss 510 NLO Axiovert 200M Tsunami microscope equipped with 488 and 633 nm lasers. For experiments involving the use of dynasore, cells were plated as described above. 24 hours prior to incubation with phage, cell culture media was replaced with 1 mL 80 μM dynasore in FBS-free cell culture media. At the time of phage incubation, the media was removed, cells were washed once with PBS, and phage were added at 0.8 nM in PBS containing 80 μM dynasore. After 1 h incubation, cells were washed twice with PBS, and 1 mL 80 μM dynasore in phenol red- and FBS-free cell culture media was added. Imaging was performed approximately 30 min – 1 h following washes. For co-localization experiments with phage and anti-fd antibodies, following incubation of cells with phage, cells were fixed with 10% formalin for 10 min, and washed once with PBS. Cells were then permeabilized with 0.01% Triton-X, and washed once more with PBS, at which point anti-Fd was added. Cells were incubated with the antibody for 40 min, washed once with 1% FBS, and then the secondary antibody was added, incubated with the cells for 20 min, cells were then washed with 1% FBS again and imaged. Where fluorescently labeled antibody (AF568-anti-fd) was used, the secondary antibody was not used, and imaging occurred following 40 min incubation with antibody and

subsequent wash with 1% FBS. For phage binding experiments with fixed cells, prior to incubation with phage, cells were fixed with 10% formalin for 10 min, followed by a single wash with PBS.

6. <u>Preparation of xenograft models.</u> All tumor xenografts were prepared in the Preclinical Therapeutics Core Facility at UCSF using IACUC- and ACURO-approved protocols. Six-week old female nu/nu mice were purchased from Charles River Laboratories. Tumor cells for injection are cultured under sterile conditions according to ATCC recommended guidelines. At the time of xenograft preparation, tumor cells are harvested, and approximately 8 million cells per mouse injected into surgically exposed number 4 mammary fat pads with a 100 μL Hamilton syringe.

7. <u>Optical imaging.</u> All imaging experiments were conducted at the Center for Molecular and Functional Imaging at UCSF using IACUC- and ACURO-approved protocols. Optical imaging was performed using an IVIS 50 (Caliper Life Sciences) instrument. Prior to injection with imaging agents, animals were anesthetized with isoflurane, and pre-injection images acquired. 2 nmol of each agent (based on dye concentration) in 150 μL PBS was injected via tail vein. Images were acquired at the following time points: 10 min, 30 min, 1 h, 2 h, 3 h, 4 h, 5 h, 6 h, 7 h, 8 h, 24 h, 48 h, and 72 h (except where euthanasia preceded that acquisition). The first assay with a particular agent continued until it had cleared in order to determine optimal time points for *ex vivo* biodistribution.

8. <u>Generation of ^{64}Cu-labeled MS2 and MS2-PEG</u>. T19paF N87C-MS2 was produced as previously described.[21] To a 100 μM sample of protein (based on capsid monomer) in 10 mM potassium phosphate buffer, pH 7.2, was added 20 equivalents of maleimide-DOTA in DMSO. The reaction was allowed to proceed for 1 h at room temperature and was purified using a Nap 10-Sephadex size exclusion column (GE Healthcare) equilibrated with phosphate buffer, pH 6.5. For the preparation of MS2-PEG samples, PEG5k-aminophenol was synthesized and reacted with DOTA-MS2 as previously described.[20] Briefly, to DOTA-MS2 (60 μM) were added 5 equivalents of PEG5k-aminophenol, and 2.5 mM NaIO4. The reaction was allowed to proceed for 2 min at pH 6.5, and then purified immediately using a Nap 5-Sephadex size exclusion column (GE Healthcare). The extent of PEG modification was determined by using optical densitometry of a Coomassie-stained SDS-PAGE gel. For the labeling of DOTA-MS2 and DOTA-MS2-PEG samples with 64Cu, 1 mL of 0.1 M ammonium citrate buffer, pH 6.2, was added to the copper stock (33.1 mCi, ~300 μL) to generate a final volume of ~1300 μL at pH 5.5 (determined by pH paper). Each reaction tube was then charged with 400 μL of 64Cu solution and 300 μL of the DOTA-MS2 (50 μM in capsid monomer) samples, resulting in a final volume of 700 μL for each. The complexation reactions were allowed to proceed for 1.5 h at room temperature, then diluted with 300 μL of saline solution. The resulting samples were then purified using Nap 10 columns. Samples were subsequently concentrated using 10 kDa molecular weight cutoff spin concentrators (Millipore). Centrifugation was performed at 5,000 rpm for 5 min per round of concentrating until the desired volume was reached.

9. <u>PET/CT studies with 64Cu-labeled MS2 and MS2-PEG</u>. All animal procedures were performed according to a protocol approved by the UCSF Institutional Animal Care and Use Committee (IACUC). For tumor inoculation, MCF7cl18 cells were implanted in the number 4 mammary fat pad on the left side. β-estradiol pellets were implanted subcutaneously in the right flank. The imaging and biodistribution experiments were started two weeks following implantation, when the tumors were ~3 mm in diameter. The mice weighed 19-23 g. Tumor-bearing nude mice in sets of 3 animals per study group were injected with 250-350 μCi of ^{64}Cu-labeled DOTA-MS2 capsids (with PEG and without PEG) in 100 μL of PBS. As a control experiment, one group was injected with free ^{64}Cu in 150 μL of PBS. One animal from each group was selected for imaging with microPET/CT (Siemens Inveon microPET docked with microCT). Dynamic imaging was performed from the time of injection (t = 0 h) to 1 h, then 20 min static scans were run at the 4 h and 8 h points, followed by a 30 min static scan at 24 h. Each PET scan was followed by the acquisition of a CT scan for registration purposes. Images were reconstructed with CT-based attenuation using the manufacturer-provided ordered subsets expectation maximization (OS-EM) algorithm resulting in 128x128x159 matrices with a voxel size of 0.776x0.776x0.796 mm3, decay corrected, and generated using Amide software. After a post-injection period of 24 h, all mice were euthanized and dissected. Blood, tumor, and major organs were collected and weighed. The

radioactivity present in each sample was determined using a gamma-counter (Wizard, Perkin Elmer) by measuring against standards of known activity generated from the respective samples. All values were decay corrected, and the percentage injected dose per gram (%ID/g) was calculated for each tissue from each mouse. Averages and standard deviations were obtained within each group.

KEY RESEARCH ACCOMPLISHMENTS:

1. Generation of phage targeting cell-surface glycoprotein CD44, receptor tyrosine-protein kinase HER3, and cell surface enzyme CD73 via infection and growth in *E. coli*.
2. Successful modification of anti-CD44, -HER3 and -CD73 phage pVIII coat proteins via pyridoxal 5'-phosphate (PLP) mediated transaminations followed by appendage of fluorophores and confirmation of binding abilities of the modified phage in breast cancer cell lines using flow cytometry and confocal microscopy.
3. Evaluation of phage uptake mechanisms via dynasore inhibition of clathrin-mediated endocytosis using confocal microscopy.
4. Confirmation of retention of phage structure following cellular internalization using co-localization of phage and anti-fd antibodies in confocal microscopy assay.
5. Confirmation of phage binding to fixed cells (as precursor to imaging with cell button sections/tumor surrogates) using confocal microsopy.
6. Established dual mammary fat pad orthotopic tumors using MCF-7 clone 18 and MDA-MB-231 cells, and performed optical imaging experiments with anti-HER2, anti-HER3, anti-CD44, and anti-CD73 phage.
7. Initial evaluation of MS2 and PEGylated-MS2 icosahedral bacteriophage as a potential alternative strategy via PET-CT imaging and bio-distribution with ^{64}Cu.

REPORTABLE OUTCOMES: Provide a list of reportable outcomes that have resulted from this research to include:

Manuscript in publication:

1. Carrico, Z. M.*; Farkas, M. E.*; Yu, Z.; Hsiao, S. C.; Marks, J. D.; Chokhawala, H.; Clark, D. S.; Francis, M. B. **"**N-terminal Labeling of Filamentous Phage to Create Cancer Marker Imaging Agents." *ACS Nano*. **2012**. *6*, 6675-6680.

Oral presentation:

1. Farkas, M. E.; Gray, J. M.; Francis, M. B. "Chemically Modified Bacteriophage as a Streamlined Approach Toward Non-Invasive Breast Cancer Imaging." **245th National Meeting of the American Chemical Society**, Philadelphia, PA, August 2012.

Poster presentations:

1. Farkas. M. E.; Carrico, Z. M.; Tong, G. J.; Wu, W.; Behrens, C. R.; Gray, J. M.; Francis, M. B. "Chemically Modified Bacteriophage as a Streamlined Approach Toward Non-Invasive Breast Cancer Imaging." **Gordon Conference in Mammary Gland Biology**, Newport, RI, June 2011

2. Farkas. M. E.; Carrico, Z. M.; Tong, G. J.; Wu, W.; Behrens, C. R.; Gray, J. M.; Francis, M. B. "Chemically Modified Bacteriophage as a Streamlined Approach Toward Non-Invasive Breast Cancer Imaging." **Department of Defense Breast Cancer Research Program 6th Era of Hope Conference**, Orlando, FL, August 2011
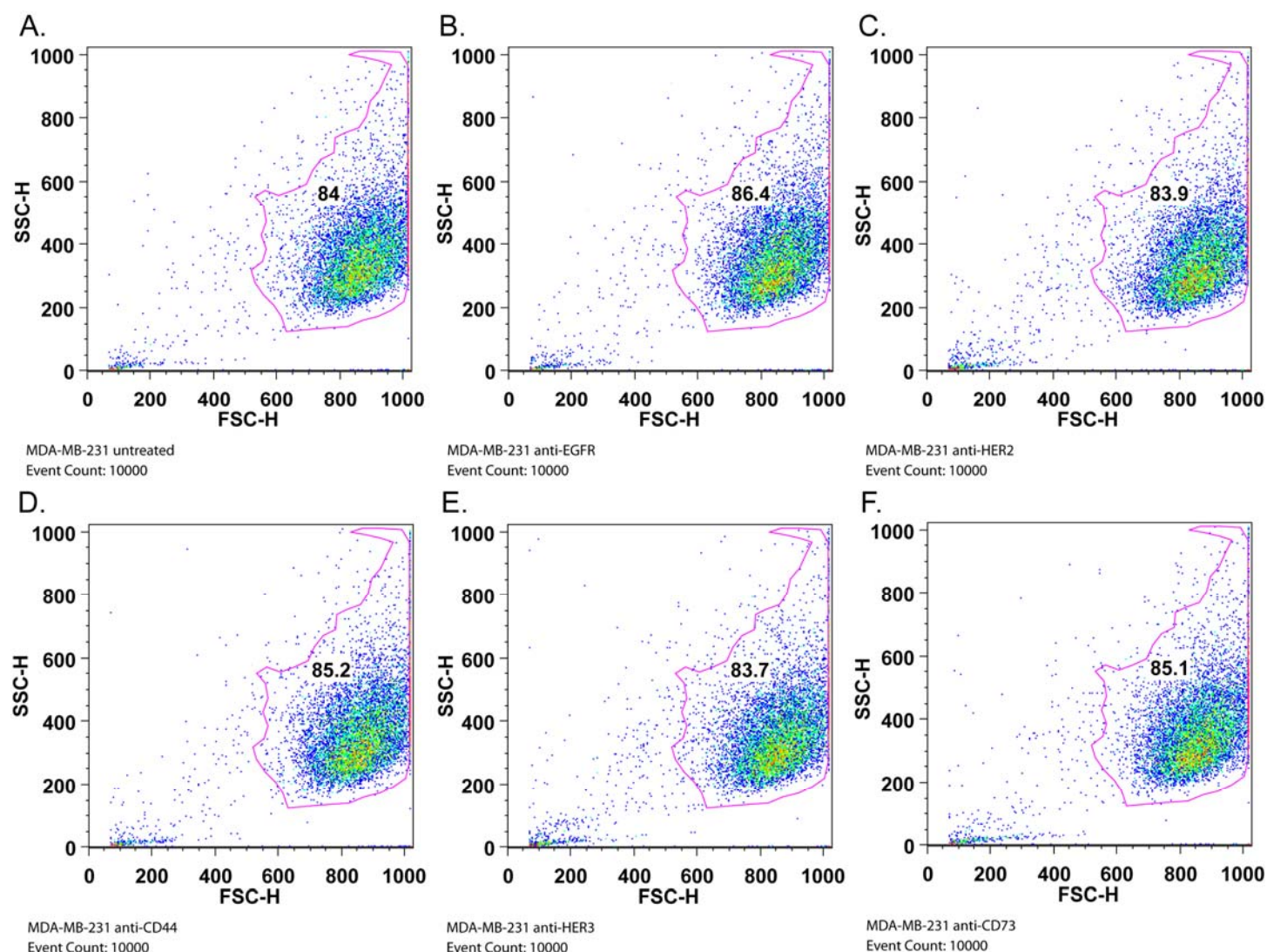
CONCLUSION: During the second year of research, I have successfully generated and selectively modified filamentous phage targeting additional cell surface markers, including CD44, HER3, and CD73, to display various levels of fluorophores. These agents have been demonstrated to specifically bind to a panel of cell lines possessing varying levels receptors *in vitro* via flow cytometry and confocal microscopy assays. The mechanisms by which phage are internalized by cells and retention of their structures upon endocytosis were assayed, along with confirmation of their abilities to bind to fixed cells possessing their respective targeted markers. Evaluation of non-specific binding and serum stability is pending, and will be assessed via size exclusion chromatography (SEC). Dual orthotopic tumors implanted in opposite mammary fat pads were generated using MCF-7 clone 18 and MDA-MB-231 cells. Optical imaging studies were performed using HER2, HER3, CD44, and CD73 phage however results were similar to those previously obtained, likely due to fluorophore quenching and unknown fate of the phage *in vivo*, resulting in enhanced liver and bladder signals. In order to remedy this situation, we are evaluating the possibility of labeling phage with ^{64}Cu radionuclides, which would allow us to utilize PET imaging, characterize agents *ex vivo*, and not be quenched. As an potential alternative to using filamentous phage, initial biodistribution experiments using icosahedral bacteriophage MS2 and PEGylated MS2 were performed using PET-CT and gamma counting assays. These agents were found to remain in the bloodstream for over 24 hours, and require further evaluation.

REFERENCES:

1. Arap, W.; Haedicke, W.; Bernasconi, M.; Kain, R.; Rajotte, D.; Krajewski, S.; Ellerby, H. M.; Bredesen, D. E.; Pasqualini, R.; Ruoslahti, E. Targeting the prostate for destruction through a vascular address. *Proc. Natl. Acad. Sci. U. S. A.* **2002**. *99,* 1527-1531.
2. Newton-Northup, J. R.; Figueroa, S. D.; Quinn, T. P.; Deutscher, S. L. Bifunctional phage-based pretargeted imaging of human prostate carcinoma. *Nucl. Med. Biol.* **2009**. *36,* 789-800.
3. Kelly, K. A.; Waterman, P.; Weissleder, R. In vivo imaging of molecularly targeted phage. *Neoplasia.* **2006**. *8,* 1011-1018.
4. Yacoby, I.; Benhar, I. Targeted filamentous bacteriophages as therapeutic agents. *Expert Opin. Drug Deliv.* **2008**. *5,* 321-329.
5. Heitner, T.; Moor, A.; Garrison, J. L.; Marks, C.; Hasan, T.; Marks, J. D. Selection of cell binding and internalizing epidermal growth factor receptor antibodies from a phage display library. *J. Immunol. Methods.* **2001**. *248,* 17-30.
6. Poul, M. A.; Becerril, B.; Nielsen, U. B.; Morisson, P.; Marks, J. D. Selection of tumor-specific internalizing human antibodies from phage libraries. *J. Mol. Biol.* **2000**. *301,* 1149-1161.
7. Amersdorfer, P.; Marks, J. D. Phage libraries for generation of Anti-Botulinum scFv antibodies. *Methods Mol. Biol.* **2000**. *145,* 219-240.
8. Chiu, C. G.; Masoudi, H.; Leung, S.; Voduc, D. K.; Gilks, B.; Huntsman, D. G.; Wiseman, S.M. HER-3 Overexpression is prognostic of reduced breast cancer survival: a study of 4046 patients. *Ann. Surg.* **2010**. *251,* 1107-1116.
9. Lopez, J. I.; Camenisch, T. D.; Stevens, M. V.; Sands, B. J.; McDonald, J.; Schroeder, J. A.; CD44 attenuates metastatic invasion during breast cancer progression. *Cancer Res.* **2005.** *65,* 6755-6763.
10. Fillmore, C.; Kuperwasser, C. Human breast cancer stem cell markers CD44 and CD24: enriching for cells with functional properties in mice or in man? *Breast Cancer Res.* **2007.** *9,* 303.
11. Zhi, X.; Wang, Y.; Zhou, X.; Yu, J.; Jian, R.; Tang, S.; Yin, L.; Zhou, P. RNAi-mediated CD73 suppression induces apoptosis and cell-cycle arrest in human breast cancer cells. *Cancer Sci.* **2010,** *101,* 2561-2569.
12. Stagg, J.; Divisekera, U.; McLaughlin, N.; Sharkey, J.; Pommey, S.; Denoyer, D.; Dwyer, K. M.; Smyth, M. J. Anti-CD73 antibody therapy inhibits breast tumor growth and metastasis. *Proc. Natl. Acad. Sci. U.S.A.,* **2010,** *107,* 1547-1552.
13. Zhou, Y.; Marks, J. D. Identification of target and function specific antibodies for effective drug delivery. *Therapeutic Antibodies: Methods and Protocols.* **2009**. *525,* 145-160.
14. Carrico, Z. M.; Farkas, M. E.; Yu, Z., Hsiao, S. C.; Marks, J. D.; Chokhawala, H.; Clark, D. S.; Francis, M. B. N-Terminal Labeling of Filamentous Phage to Create Cancer Marker Imaging Agents. *ACS Nano.* **2012.** *6,* 6675-6680.
15. O'Riordan, C.R.; Lachapelle, A.; Delgado, C.; Parkes, V.; Wadsworth, S.C.; Smith, A.E.; Francis, G.E. PEGylation of Adenovirus with Retention of Infectivity and Protection from Neutralizing Antibody In Vitro and In Vivo. *Hum. Gene. Ther.,* **1999**, *10*, 1349-1358.
16. Caliceti, P.; Veronese, F.M. Pharmacokinetic and Biodistribution Properties of Poly(Ethylene Glycol)-Protein Conjugates. *Adv. Drug Deliv. Rev.,* **2003**, *55*, 1261-1277.
17. Owens, D.E.; Peppas, N.A. Opsonization, Biodistribution, and Pharmacokinetics of Polymeric Nanoparticles. *Int. J. Pharm.*, **2006,** *307,* 93-102.
18. Belsches-Jablonski, A. P.; Biscardi, J. S.; Peavy, D. R.; Tice, D. A.; Romney, D. A.; Parsons, S. J. Src Family Kinases and HER2 Interactions in Human Breast Cancer Cell Growth and Survival. *Oncogene,* **2001**, *20*, 1465-1475.
19. Kirchhausen, T.; Macia, E.; Pelish, H. E. Use of Dynasore, the Small Molecule Inhibitor of Dynamin, in the Regulation of Endocytosis. *Methods Enzymol.,* **2008**, *438*, 77-93.
20. Behrens, C. R.; Hooker, J. M. ; Obermeyer, A. C.; Romanini, D. W.; Katz, E. M.; Francis, M. B. Rapid Chemoselective Bioconjugation Through the Oxidative Coupling of Anilines and Aminophenols. *J. Am. Chem. Soc.* **2011**, *133*, 16398-16401.

21. Stephanopoulos, N.; Carrico, Z. M.; Francis, M. B. <u>Nanoscale Integration of Sensitizing Chromophores and Porphyrins with Bacteriophage MS2.</u> *Angew. Chem. Int. Ed.,* **2009**, *48*, 9498-9502.

Supporting information:

Figure S1. Forward- and side-scatter plots for flow cytometry with MDA-MB-231 cells. Plots are shown for (**A**) untreated, (**B**) anti-EGFR phage treated, (**C**) anti-HER2 phage treated, (**D**) anti-CD44 treated, (**E**) anti-HER3 treated, and (**F**) anti-CD73 treated cells. Gating used for histogram generation (**Figure 2A**) is indicated by the pink outline. Number inside of the plot reflects percentage of cells within each gate.
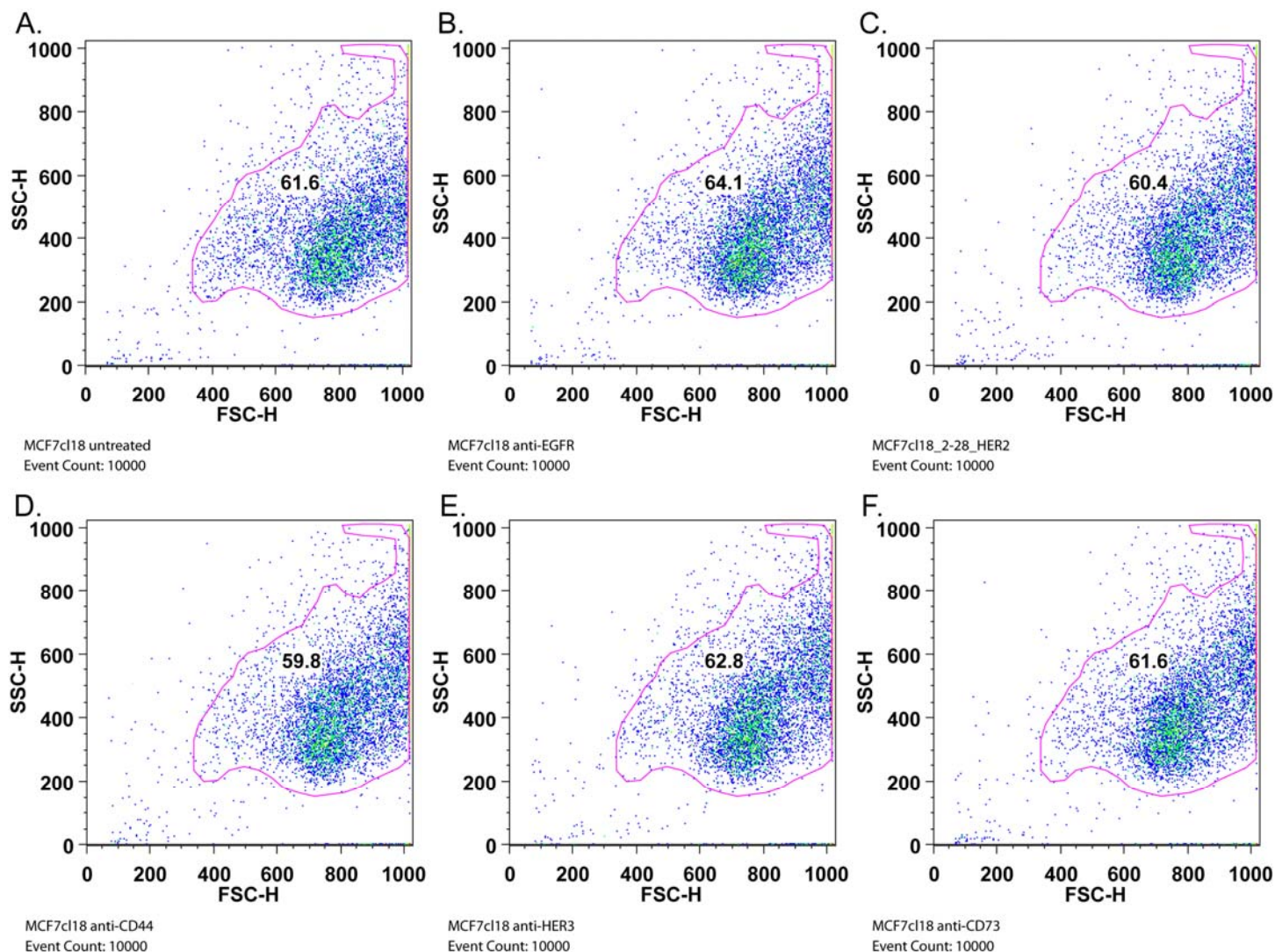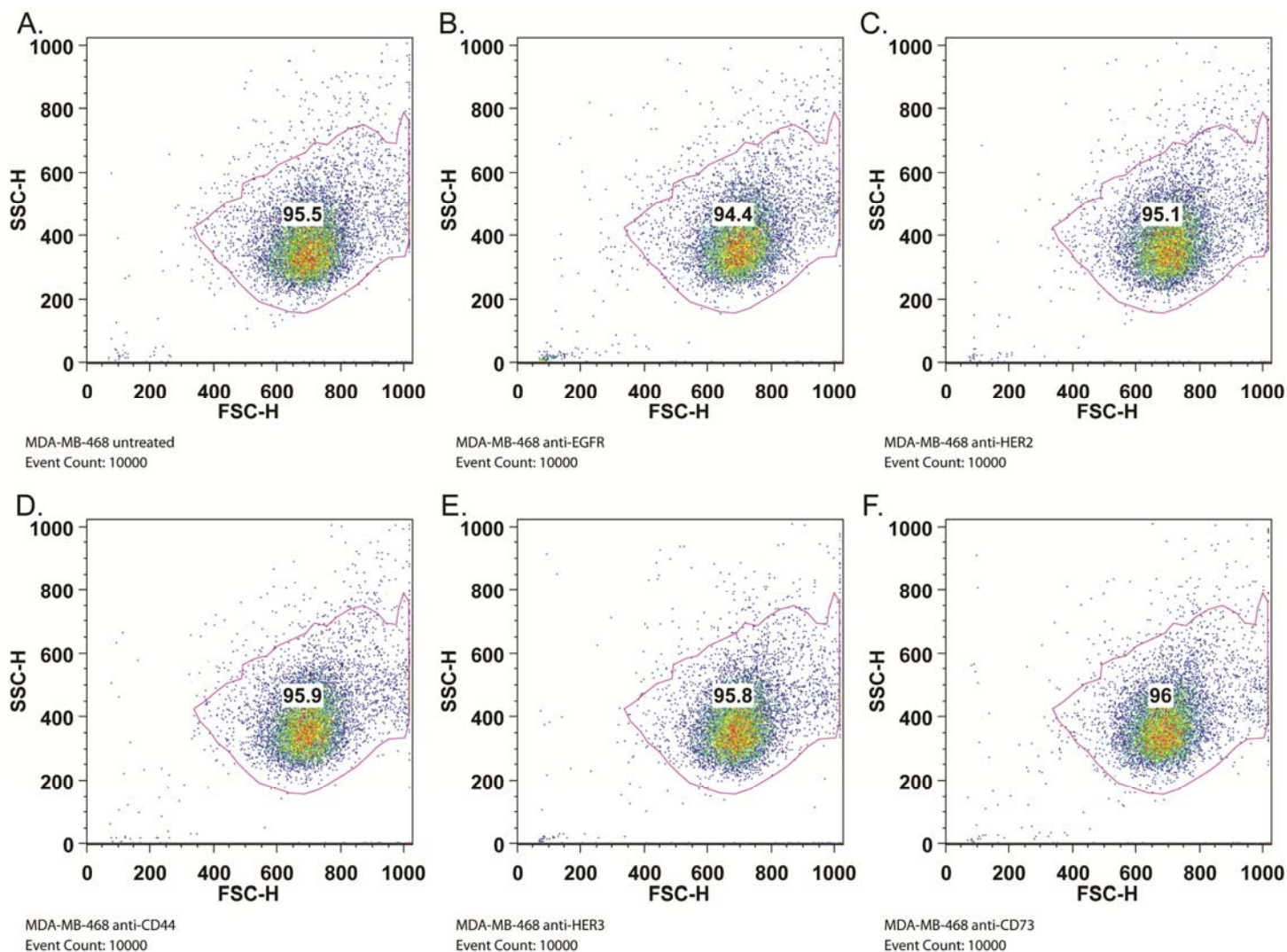
Figure S2. Forward- and side-scatter plots for flow cytometry with MCF-7 clone 18 cells. Plots are shown for (**A**) untreated, (**B**) anti-EGFR phage treated, (**C**) anti-HER2 phage treated, (**D**) anti-CD44, (**E**) anti-HER3 treated, and (**F**) anti-CD73 treated cells. Gating used for histogram generation (**Figure 2B**) is indicated by the pink outline. Number inside of the plot reflects percentage of cells within each gate.
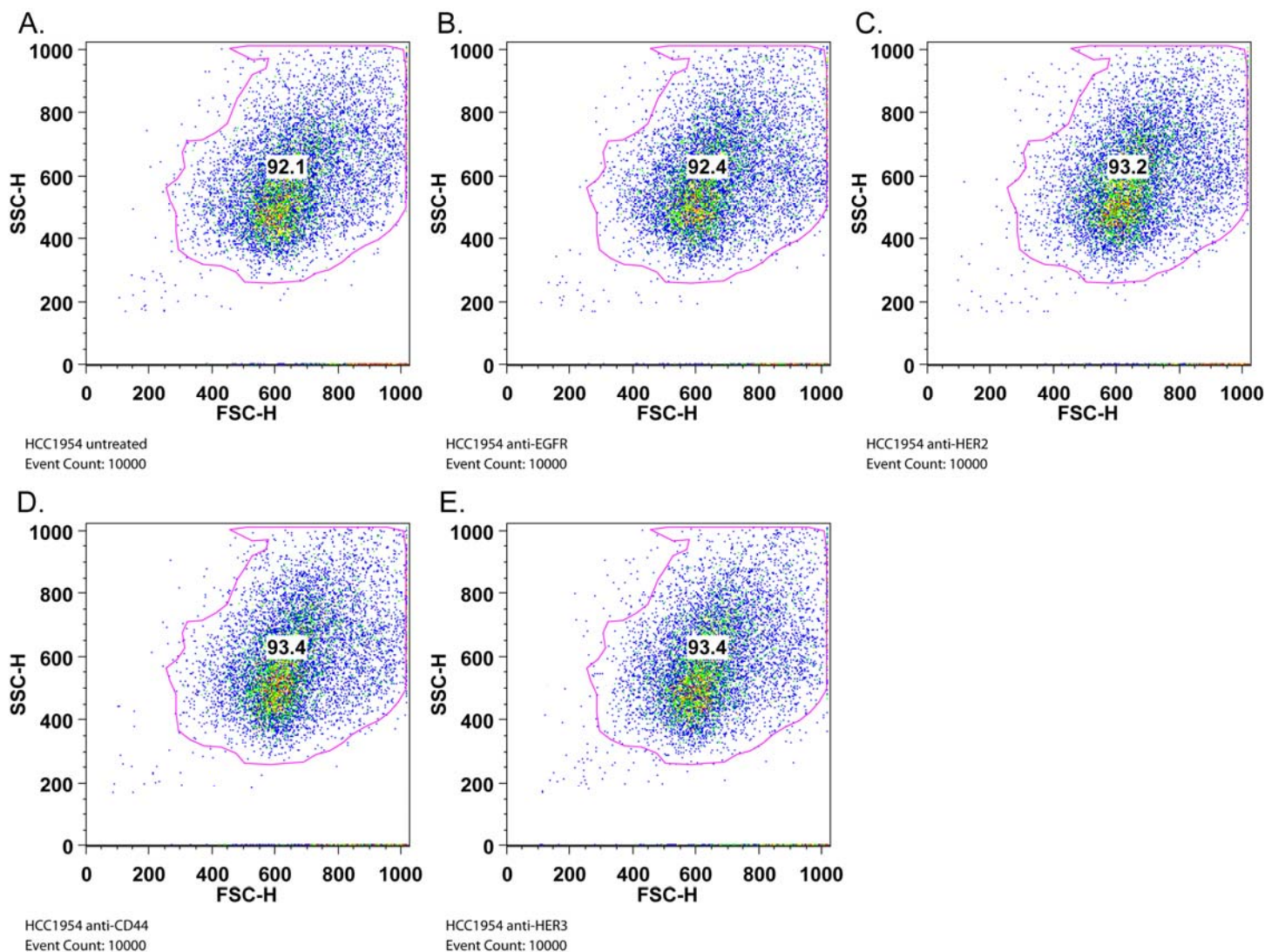
Figure S3. Forward- and side-scatter plots for flow cytometry with HCC1954 cells. Plots are shown for (**A**) untreated, (**B**) anti-EGFR phage treated, (**C**) anti-HER2 phage treated, (**D**) anti-CD44, and (**E**) anti-HER3 treated cells. Gating used for histogram generation (**Figure 2C**) is indicated by the pink outline. Number inside of the plot reflects percentage of cells within each gate.

Figure S4. Forward- and side-scatter plots for flow cytometry with MDA-MB-468 cells. Plots are shown for (**A**) untreated, (**B**) anti-EGFR phage treated, (**C**) anti-HER2 phage treated, (**D**) anti-CD44 treated, (**E**) anti-HER3 treated, and (**F**) anti-CD73 treated cells. Gating used for histogram generation (**Figure 2D**) is indicated by the pink outline. Number inside of the plot reflects percentage of cells within each gate.
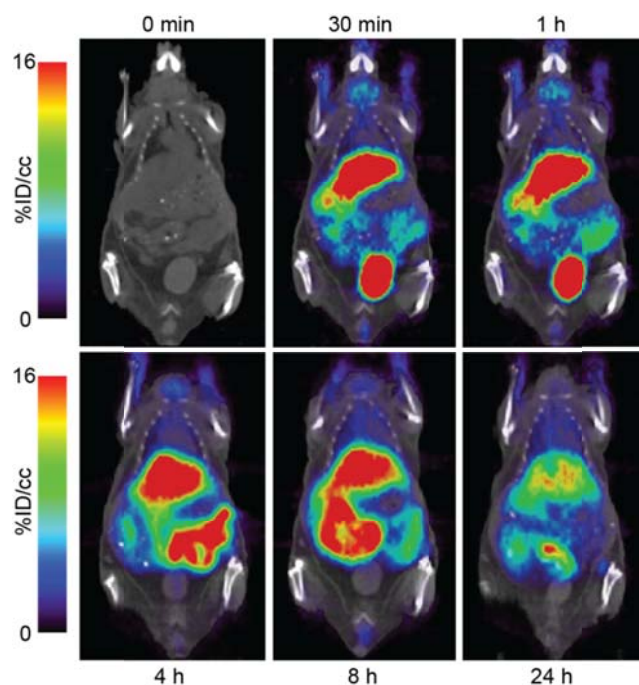
Figure S5. PET imaging of mice with ^{64}Cu (control). PET-CT images from a mouse imaged with ^{64}Cu. A dynamic scan was performed over the first 60 min, 24followed by scans obtained at 4, 8, and 24 h. All images have been decay-corrected and normalized. The scales are reported as percent injected dose per milliliter (%ID/cc).

N-Terminal Labeling of Filamentous Phage To Create Cancer Marker Imaging Agents

Zachary M. Carrico,[†,⊥] Michelle E. Farkas,[†,⊥] Yu Zhou,[‡] Sonny C. Hsiao,[†] James D. Marks,[‡]
Harshal Chokhawala,[§] Douglas S. Clark,[§] and Matthew B. Francis[†,*]

[†]Department of Chemistry, University of California, Berkeley, California 94720, United States, [‡]Department of Anesthesia and Pharmaceutical Chemistry, University of California, San Francisco, California 94143, United States, and [§]Department of Chemical Engineering, University of California, Berkeley, California 94720, United States. [⊥]These authors contributed equally to this work.

Through the use of molecular diversity techniques, filamentous phage can be evolved to bind proteins, polymers, small molecules, and metal ions with high affinity and selectivity.[1] The success of this platform is due to the ability of filamentous phage to express a wide variety of peptides and proteins as extensions of the p3 and p8 coat proteins that comprise the capsid (Figure 1). This method has provided useful binders for a variety of research efforts in molecular biology, biotechnology, biomedicine, and materials science.[2] In addition, the body of the phage has also proven useful as a robust scaffold for nanoparticle nucleation,[3] electrode templating,[4] light collection,[5] cell growth and differentiation,[6] and drug delivery.[7] To enhance these capabilities, we describe herein a convenient N-terminal-selective modification method that can introduce synthetic functionality on the phage coat proteins without interfering with their binding abilities. We demonstrate the utility of this technique by directly converting evolved phage into targeted imaging agents for *in vitro* cell targeting experiments. Furthermore, we use this method to attach up to 3000 polymer chains to these structures without compromising their ability to recognize specific receptors on live cells—a useful capability for reducing background binding and a likely requirement for developing future phage-based agents for *in vivo* applications.

Filamentous phage, such as M13 and fd, have approximately five copies of each of their minor coat proteins (p3, p6, p7, and p9, Figure 1). In addition, fd and M13 phage have 4200 and 2700 copies of the major coat protein (p8), respectively.[2] The p3 sites serve as the principal locations for

ABSTRACT
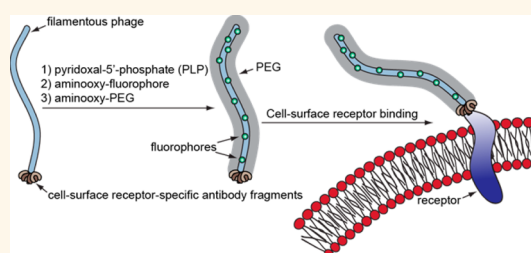
We report a convenient new technique for the labeling of filamentous phage capsid proteins. Previous reports have shown that phage coat protein residues can be modified, but the lack of chemically distinct amino acids in the coat protein sequences makes it difficult to attach high levels of synthetic molecules without altering the binding capabilities of the phage. To modify the phage with polymer chains, imaging groups, and other molecules, we have developed chemistry to convert the N-terminal amines of the ~4200 coat proteins into ketone groups. These sites can then serve as chemospecific handles for the attachment of alkoxyamine groups through oxime formation. Specifically, we demonstrate the attachment of fluorophores and up to 3000 molecules of 2 kDa poly(ethylene glycol) (PEG2k) to each of the phage capsids without significantly affecting the binding of phage-displayed antibody fragments to EGFR and HER2 (two important epidermal growth factor receptors). We also demonstrate the utility of the modified phage for the characterization of breast cancer cells using multicolor fluorescence microscopy. Due to the widespread use of filamentous phage as display platforms for peptide and protein evolution, we envision that the ability to attach large numbers of synthetic functional groups to their coat proteins will be of significant value to the biological and materials communities.

KEYWORDS: phage display · bioorthogonal · bioconjugation · materials science · cancer imaging

molecular evolution, especially for large protein inserts such as single-chain antibody variable fragments (scFvs) and enzymes. This leaves the p8 sites as abundant locations for the attachment of additional molecules. To introduce synthetic components into these assemblies, the covalent modification of filamentous phage has typically been accomplished through the
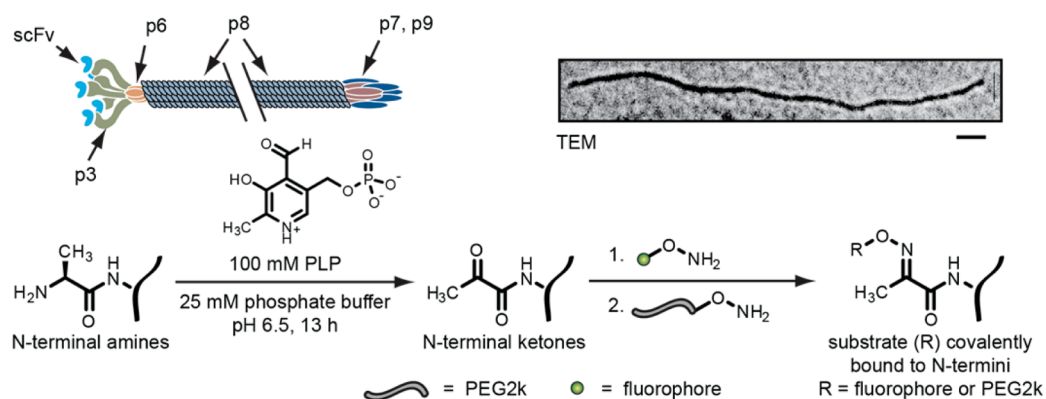
Figure 1. Cartoon (above) and chemical scheme (below) for the transamination of filamentous phage and the attachment of synthetic molecules. The N-termini are transaminated to yield ketone-bearing proteins, which are then reacted with aminooxy-functionalized fluorophores (green circles), followed by aminooxy-functionalized PEG2k (gray strands). The double slash indicates that the phage is much longer than shown when scaled to the minor coat proteins. The TEM image was stained with uranyl acetate (top right, scale bar represents 100 nm).

nonspecific modification of amine groups on the capsid surfaces with NHS esters.[8,9] However, this approach also leads to extensive acylation of the many lysine residues on the p3 proteins and their associated protein fusions, adding considerable heterogeneity and possible binding interference at high modification levels. Tyrosine residues have also been targeted on the phage surface through the use of diazonium coupling reactions,[10] but this approach is also expected to lead to significant modification of critical residues in the evolved proteins. Methods requiring the genetic modification of phage DNA have been attempted to increase specificity. In one case, serine or threonine was genetically introduced at p3 N-termini and oxidized with sodium periodate to produce an aldehyde for chemical labeling.[11] This was not demonstrated for the major coat protein p8 and requires use of sodium periodate, which can undesirably oxidize cysteines. Enzymatic ligations offer another genetic approach, as demonstrated with biotin ligase[12] and sortase A.[13,14] These techniques offer more specificity than prior chemical-labeling approaches, but they also require genetic engineering of phage DNA, which may be undesired or unfeasible in certain contexts. Our goal was to develop a simple yet reliable chemical strategy that did not require prior genetic engineering.

To provide a facile, controlled method for modifying filamentous phage with hundreds or even thousands of new functional groups, we have applied a two-step transamination/oxime formation technique.[15−18] This reaction sequence has been shown to be highly selective for N-terminal groups and does not lead to the transamination of lysine ε-amines. Using high-throughput solid phase screening methods, we have previously determined that this reaction proceeds most readily when N-terminal alanine residues are present and that it can be accelerated by proximal lysine side chains.[19] The phage p8 monomers possess a solvent-exposed N-terminal alanine and a lysine at the

$i+7$ position, making this an especially promising substrate for this reaction.

This modification strategy was developed using filamentous fd phage that display single-chain antibody fragments (scFvs) on their p3 minor coat proteins. These scFvs recognize either epidermal growth factor receptor (EGFR) or human epidermal growth factor receptor 2 (HER2) and were identified using phage display.[20−22] The overexpression of these receptors is associated with many different breast cancer serotypes, thus providing a motivation for the installation of imageable groups[23,24] on these phage for use in diagnostic applications.[25] In parallel, we also used fd phage bearing an scFv targeting botulinum toxin serotype A (anti-BoNT) as a negative control.[22]

RESULTS AND DISCUSSION

To introduce ketones into the coat proteins, phage were transaminated using a 100 mM solution of pyridoxal 5′-phosphate (PLP) at pH 6.5 for 13 h. The excess PLP was then removed by precipitating the phage, after which they were exposed to various alkoxyamine compounds in pH 6.5 buffer for up to 24 h. Aniline catalysis was used to accelerate oxime formation, as has been previously reported by Dawson and coworkers.[26] The specific reaction times and alkoxyamine concentrations were selected based on the levels of modification sought. To estimate the overall extent of p8 modification, a sample of ketone-labeled fd phage was reacted with 2-(aminooxy)acetic acid. Analysis of the coat proteins was achieved using MALDI-TOF mass spectrometry, revealing that the vast majority of the p8 proteins formed the oxime product (Figure 2a and Supporting Information Figure S1), indicating that each fd phage can be loaded with thousands of molecules. Only one addition per p8 was observed, indicating N-terminal specificity even in the presence of five p8 lysines. The overall protein recovery for the transamination and oxime formation steps ranged
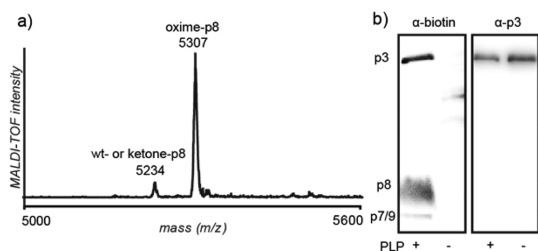
Figure 2. Analysis of filamentous phage modified with small molecules. (a) Matrix-assisted laser desorption/ionization time-of-flight (MALDI-TOF) spectrum showing p8 oxime formation following reaction with 2-(aminooxy)acetic acid (expected mass increase: 73 m/z, observed: 73 m/z). Non-transaminated fd proteins exposed to the same alkoxyamine resulted in no oxime product formation (see Supporting Information Figure S1). (b) Western blot of M13KE coat protein labeling with biotin followed by blotting with neutravidin-HRP or α-p3 antibodies. Coat protein molecular weights are as follows: p3, 46.5 kDa; p6, 12.4 kDa; p7, 3.6 kDa; p8, 5.2 kDa; p9, 3.7 kDa. Labeling of p7 and p9 cannot be distinguished due to their similar molecular weights (3.6 and 3.7 kDa, respectively). The p6 is not observed, congruent with an N-terminus inaccessible for modification.

from 55 to 95%, with 80% being a typical value. Unfortunately, despite many attempts, protein digest experiments failed to give any cleaved species for the p8 protein, presumably due to its very low solubility and propensity for aggregation once removed from the assembled structure.

The only byproduct was a small amount of a covalent adduct of the protein with the PLP, which presumably formed through an aldol addition of the N-terminal pyruvamide to the pyridoxal aldehyde group. This PLP adduct was not visible following reaction of phage with aminooxy-derivatized molecules via MALDI-TOF mass spectrometry analysis, possibly due to its poor ionization or insufficient quantity. It was, however, identified by mass spectrometry after disassembling the phage using RP-HPLC to isolate the PLP adduct-p8 from wt- and ketone-p8 species (Supporting Information Figures S2 and S3). The negative charge of the phosphate group resulted in the earlier elution via RP-HPLC. This species has been observed in transamination reactions previously, and since it possesses a ketone group, it can still participate in oxime formation.[16] This, in addition to its very low abundance, renders it insignificant for most applications.
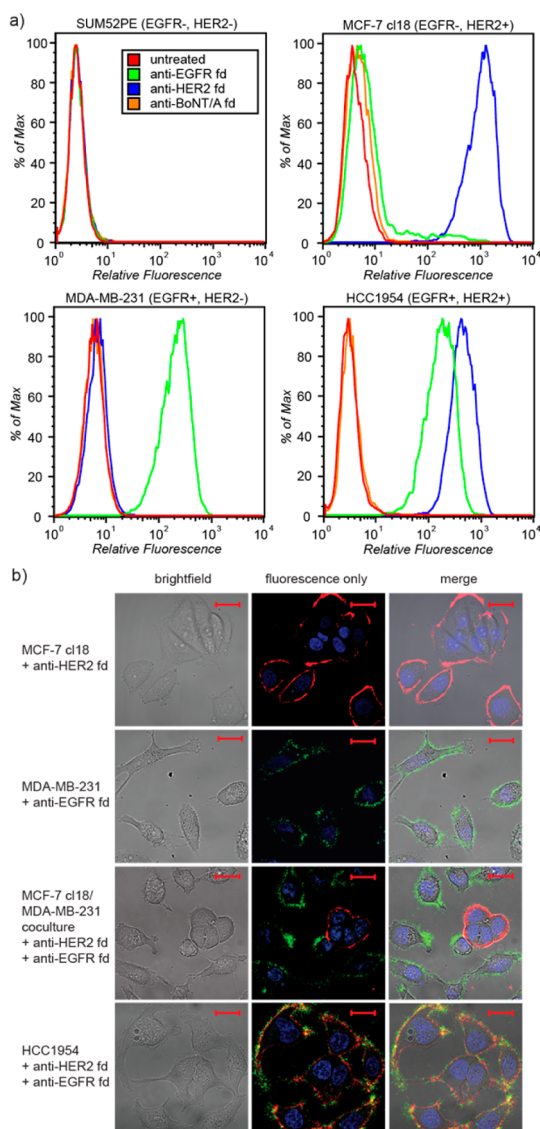
The small p3-to-p8 ratio for fd phage prevented p3 detection by mass spectrometry and Western blotting. Instead, we turned to the use of M13KE phage, which are fd analogues with smaller genomes. They require a smaller number of p8 proteins to tile the length of the phage and therefore have a higher ratio of p3 to p8 proteins. The M13KE and wt-fd coat proteins are identical, except for a single D12N point mutation in p8.[27,28] To detect the modifications with improved sensitivity, transaminated M13KE was

exposed to biotin-ONH_2 and analyzed via Western blotting with neutravidin-HRP (Figure 2b). All of the coat proteins with accessible N-termini, including p3, showed labeling. The α-p3 blot in Figure 2b shows that both lanes contain approximately the same concentration of phage, while the neutravidin-HRP (α-biotin) blot shows that only PLP-reacted phage are biotin-labeled.

To verify the ability of the modified phage to bind their targets, samples of transaminated anti-EGFR, anti-HER2, and anti-BoNT fd phage were reacted with Alexa Fluor 488 or 647 C5-aminooxyacetamide (AF488/647-ONH_2) dyes. For the cell microscopy experiments described below, approximately 6−8% of the p8 proteins (∼300 copies/phage, as determined using UV/vis) were labeled with the fluorophores. Up to 80% of the p8 proteins could be labeled using 100 mM aniline as a catalyst,[26] albeit with decreased solubility. The modified phage bound to their appropriate cell surface receptors with excellent specificity, as revealed using flow cytometry (Figure 3a and Supporting Information Figures S4−S7). The negative control anti-BoNT phage showed no binding. In terms of cell viability, these data also indicated that only 0.25 to 3.0% of the cells had died during the exposure to the phage-based imaging agents, which was in line with untreated cell samples.

The selective binding capabilities of the EGFR and HER2 targeted phage were also confirmed in microscopy experiments. A panel of breast cancer cells was treated with the phage and visualized using live cell confocal microscopy. These images (Figure 3b and Supporting Information Figures S8−S12) demonstrated the retention of excellent specificities and binding capabilities of fd for their targeted receptors following chemical modification. Upon increased incubation times (>2 h), phage targeting overexpressed markers were observed to be internalized by the respective cells. Preliminary results indicate that this occurs via receptor-mediated endocytosis; however, further experiments to clarify this behavior are in progress.

The ability of these fd to image receptor overexpression in vitro, even when different cell types are mixed, portends well for their use in vivo. In anticipation of future in vivo applications, we investigated the attachment of poly(etheylene glycol) (PEG) polymers to the phage capsids. PEG has been shown to reduce nonspecific binding, decrease immunogenicity, and increase the solubility of attached molecules.[29] Ketone-labeled fd were reacted with 2 kDa O-(methoxypoly-(ethylene glycol))-hydroxylamine (PEG2k-ONH_2),[30] and the percentage of p8 proteins that were modified was quantified using RP-HPLC (Supporting Information Figure S13). By varying the reaction times, samples with differing levels of PEG2k-labeled p8s were prepared. Presumably higher concentrations of the PEG2k-ONH_2 could achieve shorter modification times,
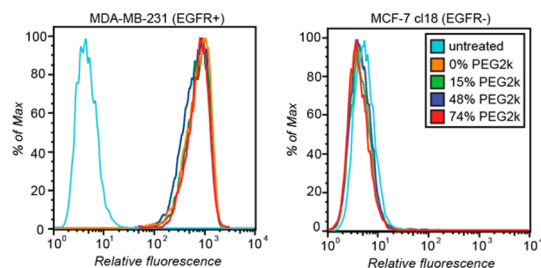
ARTICLE

Figure 4. Flow cytometry analysis of AF488-labeled anti-EGFR fd possessing various levels of PEG modifications. The target cells were MDA-MB-231 (EGFR$^+$, left), and the control cells were MCF-7 cl18 (EGFR$^-$, right). Phage concentrations were 0.8 nM. Gating data are shown in Supporting Information Figure S16. As a negative control, anti-BoNT fd labeled with nearly identical levels of PEG showed no binding (see Supporting Information Figures S17 and S18).

Figure 3. Fluorophore-modified fd phage cell binding results. (a) Flow cytometry with AF488-labeled phage (applied at 0.8 nM) indicated selective recognition of EGFR and HER2 epitopes. The legend for all histograms is shown in SUM52PE inset. Gating data are shown in Supporting Information Figures S4—S7. (b) Live cell confocal microscopy images of fluorescently labeled anti-HER2 and anti-EGFR fd showed marker-specific binding to breast cancer cell lines. Fluorescence is as follows: DAPI (blue), anti-HER2 fd (red), anti-EGFR fd (green). Scale bars represent 20 μm. Control and larger images with all fluorescence channels are shown in Supporting Information Figures S8—S12.

but we avoided using them to prevent precipitation of the phage. For phage labeled with fluorophores, there were no observed changes in the absorption or emission properties of the dyes upon addition of

the chains. The added PEG chains also caused no morphological changes that could be observed by TEM (Supporting Information Figure S14).

Zeta-potential measurements were obtained in order to determine the ability of the PEG polymers to shield fd charge (Supporting Information Figure S15). An increase in negative charge was noted following PLP modification, presumably due to the loss of the cationic N-terminal amino groups on the p8 monomers. As anticipated, the negative charge decreased with increasing levels of PEG modification. At 67% p8 labeling, the zeta-potential was -5.5 ± 7.3 mV, nearly an order of magnitude less than that of ketone-labeled fd. The binding abilities of PEG-labeled fd were also evaluated by flow cytometry (Figure 4 and Supporting Information Figures S16—S18). The PEG-labeled anti-EGFR fd continued to bind MDA-MB-231 (EGFR positive) cells, while none bound the MCF-7 cl18 cells (EGFR negative).

SUMMARY

The chemical modifications to fd phage described herein were used to produce highly selective fluorescent imaging agents that can be readily adapted for use with MRI, PET, and other detection modalities. Furthermore, the binding molecule, phage length, and labeling molecule type can be adjusted for a variety of *in vitro* and *in vivo* applications.[31] By combining the ability of phage display to obtain genetically encodable binding molecules with the N-terminal transamination/oximation method for appending chemical functionality, a much wider variety of well-defined multifunctional materials can now be accessed.

METHODS

Unless otherwise noted, all chemical reagents were purchased from Aldrich. Alexa Fluor 488 and 647 C5-aminooxyacetamide, bis(triethylammonium) salt, N-(aminooxyacetyl)-

N′-(D-biotinoyl) hydrazine, trifluoroacetic acid, salt, and neutravidin-HRP were purchased from Invitrogen. Anti-M13 p3 was purchased from New England Biolabs. O-(Methoxypoly-(ethylene glycol))-hydroxylamine (PEG2k-ONH$_2$) was prepared as previously described.[30] Cells were maintained according to

ATCC recommended guidelines. For specific instrumentation and detailed experimental information, see the Supporting Information.

Fd Production. Fd displaying anti-EGFR, -HER2, and -BoNT scFvs used in these experiments have been reported previously[20−22] and were generated using standard techniques.[32]

Transamination. Fd (75−128 nM) were transaminated using 100 mM PLP in 25 mM phosphate buffer at pH 6.5 for 13 h at room temperature. Excess PLP was removed *via* a series of precipitations with 20% PEG8k/2.5 M NaCl, supernatant removal, and resuspension in PBS.

Reaction with Biotin and Western Blotting. The final reaction concentrations were 296 nM M13KE, 10 mM phosphate buffer (pH 6.2), 10 mM aniline, and 16 mM biotin-ONH$_2$. After 15 h at room temperature, the reaction was quenched by adding D,L-glyceraldehyde to a final concentration of 33.3 μM, followed by SDS-PAGE. A 1:10 000 dilution of anti-p3 and a 1:2000 dilution of Neutravidin-HRP were used for blotting experiments. A Genscript 1 h western kit was used for detection.

Reaction with 2-(Aminooxy)acetic Acid. Twenty-four nanomolar fd was reacted with 5 mM 2-(aminooxy)acetic acid in 100 mM anilinium acetate, pH 4.7, for 21 h at room temperature. Reaction conditions were different from those used for other labeling reactions because the objective of this experiment was to estimate the percentage of transaminated p8s. For this reason, low pH and high aniline concentrations were used to maximize p8 labeling. Other experiments used higher pH values and lower aniline concentrations to better control the percent of p8s modified.

Reaction with Fluorophores. The final reaction concentrations were 185 nM fd, 20 mM phosphate buffer (pH 6.2), 10 mM (for AF488) or 100 mM aniline (for AF647), and 1 mM AF488/647-ONH$_2$. Exposure to these conditions for 45 min at room temperature resulted in 2% p8 modification (for phage to be reacted with PEG subsequently). Otherwise, reactions continued for 16−18 h at room temperature, resulting in 6−8% levels of dye modification. After the reaction, the excess fluorophore was removed using the purification described above.

Flow Cytometry. Five hundred thousand cells in 100 μL of 1% FBS/DPBS were mixed with 100 μL of 0.8 nM fd and incubated at 4 °C. After 1 h, each sample was diluted to 1 mL with 1% FBS/DPBS, and the cells were washed before resuspending in 200 μL of 1% FBS/DPBS.

Cell Microscopy. Two milliliters of 25 000 cells/mL in 35 mm glass bottom dishes (Mattek) was grown at 37 °C with 5% CO$_2$ for 72−96 h. The cells were washed with PBS, and 150 μL of 0.8 nM fd in 1% FBS/DPBS was added before incubating at 37 °C with 5% CO$_2$ for 1 h. The cells were washed three times with PBS followed by addition of 1 mL of phenol-red-free media with 10% FBS. DAPI was added to 1 μM prior to imaging.

Reaction with PEG2k. Thirty-seven nanomolar fd, 20 mM PEG2k-ONH$_2$, 20 mM phosphate buffer (pH 6.2), and 10 mM aniline were combined. Following the appropriate reaction times, samples were washed over an Illustra Nap-5 gel filtration column, eluting with PBS.

Conflict of Interest: The authors declare no competing financial interest.

Supporting Information Available: Full characterization of conjugates, chromatograms, and additional flow cytometry data are provided. This material is available free of charge *via* the Internet at http://pubs.acs.org.

REFERENCES AND NOTES

1. Smith, G. P.; Petrenko, V. A. Phage Display. *Chem. Rev.* **1997**, *97*, 391–410.

2. Kehoe, J. W.; Kay, B. K. Filamentous Phage Display in the New Millennium. *Chem. Rev.* **2005**, *105*, 4056–4072.

3. Mao, C. B.; Solis, D. J.; Reiss, B. D.; Kottmann, S. T.; Sweeney, R. Y.; Hayhurst, A.; Georgiou, G.; Iverson, B.; Belcher, A. M. Virus-Based Toolkit for the Directed Synthesis of Magnetic and Semiconducting Nanowires. *Science* **2004**, *303*, 213–217.

4. Lee, Y. J.; Yi, H.; Kim, W. J.; Kang, K.; Yun, D. S.; Strano, M. S.; Ceder, G.; Belcher, A. M. Fabricating Genetically Engineered High-Power Lithium-Ion Batteries Using Multiple Virus Genes. *Science* **2009**, *324*, 1051–1055.

5. Nam, Y. S.; Shin, T.; Park, H.; Magyar, A. P.; Choi, K.; Fantner, G.; Nelson, K. A.; Belcher, A. M. Virus-Templated Assembly of Porphyrins into Light-Harvesting Nanoantennae. *J. Am. Chem. Soc.* **2010**, *132*, 1462–1463.

6. Merzlyak, A.; Indrakanti, S.; Lee, S.-W. Genetically Engineered Nanofiber-like Viruses for Tissue Regenerating Materials. *Nano Lett.* **2009**, *9*, 846–852.

7. Arap, W.; Pasqualini, R.; Ruoslahti, E. Cancer Treatment by Targeted Drug Delivery to Tumor Vasculature in a Mouse Model. *Science* **1998**, *279*, 377–380.

8. Yacoby, I.; Benhar, I. Targeted Filamentous Bacteriophages as Therapeutic Agents. *Expert Opin. Drug Delivery* **2008**, *5*, 321–329.

9. Hilderbrand, S. A.; Kelly, K. A.; Niedre, M.; Weissleder, R. Near Infrared Fluorescence-Based Bacteriophage Particles for Ratiometric pH Imaging. *Bioconjugate Chem.* **2008**, *19*, 1635–1639.

10. Li, K.; Chen, Y.; Li, S.; Nguyen, H. G.; Niu, Z.; You, S.; Mello, C. M.; Lu, X.; Wang, Q. Chemical Modification of M13 Bacteriophage and Its Application in Cancer Cell Imaging. *Bioconjugate Chem.* **2010**, *21*, 1369–1377.

11. Ng, S.; Jafari, M. R.; Matochko, W. L.; Derda, R. Quantitative Synthesis of Genetically Encoded Glycopeptide Libraries Displayed on M13 Phage. *ACS Chem. Biol.* **2012**, 10.1021/cb300187t.

12. Chen, I.; Choi, Y.-A.; Ting, A. Y. Phage Display Evolution of a Peptide Substrate for Yeast Biotin Ligase and Application to Two-Color Quantum Dot Labeling of Cell Surface Proteins. *J. Am. Chem. Soc.* **2007**, *129*, 6619–6625.

13. Hess, G. T.; Cragnolini, J. J.; Popp, M. W.; Allen, M. A.; Dougan, S. K.; Spooner, E.; Ploegh, H. L.; Belcher, A. M.; Guimaraes, C. P. M13 Bacteriophage Display Framework That Allows Sortase-Mediated Modification of Surface-Accessible Phage Proteins. *Bioconjugate Chem.* **2012**, *23*, 1478–1487.

14. Popp, M. W.; Antos, J. M.; Grotenbreg, G. M.; Spooner, E.; Ploegh, H. L. Sortagging: A Versatile Method for Protein Labeling. *Nat. Chem. Biol.* **2007**, *3*, 707–708.

15. Gilmore, J. M.; Scheck, R. A.; Esser-Kahn, A. P.; Joshi, N. S.; Francis, M. B. N-Terminal Protein Modification through a Biomimetic Transamination Reaction. *Angew. Chem., Int. Ed.* **2006**, *45*, 5307–5311.

16. Scheck, R. A.; Dedeo, M. T.; Iavarone, A. T.; Francis, M. B. Optimization of a Biomimetic Transamination Reaction. *J. Am. Chem. Soc.* **2008**, *130*, 11762–11770.

17. Dixon, H. B. F. N-Terminal Modification of Proteins. *J. Protein Chem.* **1984**, *3*, 99–108.

18. Snell, E. E. The Vitamin B$_6$ Group. V. The Reversible Interconversion of Pyridoxal and Pyridoxamine by Transamination Reactions. *J. Am. Chem. Soc.* **1945**, *67*, 194–197.

19. Witus, L. S.; Moore, T.; Thuronyi, B. W.; Esser-Kahn, A. P.; Scheck, R. A.; Iavarone, A. T.; Francis, M. B. Identification of Highly Reactive Sequences for PLP-Mediated Bioconjugation Using a Combinatorial Peptide Library. *J. Am. Chem. Soc.* **2010**, *132*, 16812–16817.

20. Zhou, Y.; Drummond, D. C.; Zou, H.; Hayes, M. E.; Adams, G. P.; Kirpotin, D. B.; Marks, J. D. Impact of Single-Chain Fv Antibody Fragment Affinity on Nanoparticle Targeting of Epidermal Growth Factor Receptor-Expressing Tumor Cells. *J. Mol. Biol.* **2007**, *371*, 934–947.

21. O'Connell, D.; Becerril, B.; Roy-Burman, A.; Daws, M.; Marks, J. D. Phage *versus* Phagemid Libraries for Generation of Human Monoclonal Antibodies. *J. Mol. Biol.* **2002**, *321*, 49–56.

27

22. Amersdorfer, P.; Wong, C.; Smith, T.; Chen, S.; Deshpande, S.; Sheridan, R.; Marks, J. D. Genetic and Immunological Comparison of Anti-Botulinum Type A Antibodies from Immune and Non-immune Human Phage Libraries. *Vaccine* **2002**, *20*, 1640–1648.

23. Hooker, J. M.; O'Neil, J. P.; Romanini, D. W.; Taylor, S. E.; Francis, M. B. Genome-Free Viral Capsids as Carriers for Positron Emission Tomography Radiolabels. *Mol. Imaging Biol.* **2008**, *10*, 182–191.

24. Datta, A.; Hooker, J. M.; Botta, M.; Francis, M. B.; Aime, S.; Raymond, K. N. High Relaxivity Gadolinium Hydroxypyridonate-Viral Capsid Conjugates: Nanosized MRI Contrast Agents. *J. Am. Chem. Soc.* **2008**, *130*, 2546–2552.

25. Milanezi, F.; Carvalho, S.; Schmitt, F. C. EGFR/HER2 in Breast Cancer: A Biological Approach for Molecular Diagnosis and Therapy. *Expert Rev. Mol. Diagn.* **2008**, *8*, 417–434.

26. Dirksen, A.; Hackeng, T. M.; Dawson, P. E. Nucleophilic Catalysis of Oxime Ligation. *Angew. Chem., Int. Ed.* **2006**, *45*, 7581–7584.

27. van Wezenbeek, P. M.; Hulsebos, T. J.; Schoenmakers, J. G. Nucleotide Sequence of the Filamentous Bacteriophage M13 DNA Genome: Comparison with Phage Fd. *Gene* **1980**, *11*, 129–148.

28. Noren, K. A.; Noren, C. J. Construction of High-Complexity Combinatorial Phage Display Peptide Libraries. *Methods* **2001**, *23*, 169–178.

29. Pasut, G.; Veronese, F. M. PEG Conjugates in Clinical Development or Use as Anticancer Agents: An Overview. *Adv. Drug Delivery Rev.* **2009**, *61*, 1177–1188.

30. Schlick, T. L.; Ding, Z.; Kovacs, E. W.; Francis, M. B. Dual-Surface Modification of the Tobacco Mosaic Virus. *J. Am. Chem. Soc.* **2005**, *127*, 3718–3723.

31. Specthrie, L.; Bullitt, E.; Horiuchi, K.; Model, P.; Russel, M.; Makowski, L. Construction of a Microphage Variant of Filamentous Bacteriophage. *J. Mol. Biol.* **1992**, *228*, 720–724.

32. Barbas, C. F.; Burton, D. R.; Scott, J. K.; Silverman, G. J. *Phage Display: A Laboratory Manual*; Cold Spring Harbor Laboratory Press: Cold Spring Harbor, NY, 2001.

28

N-terminal Labeling of Filamentous Phage to Create Cancer Marker Imaging Agents

Zachary M. Carrico,[a, ‡] Michelle E. Farkas,[a, ‡] Yu Zhou,[b] Sonny C. Hsiao,[a] James D. Marks,[b] Harshal Chokhawala,[c] Douglas S. Clark,[c] and Matthew B. Francis[a,*]

[a]Department of Chemistry, University of California, Berkeley, CA 94720, [b]Department of Anesthesia and Pharmaceutical Chemistry, University of California, San Francisco, CA 94143, and [c]Department of Chemical Engineering, University of California, Berkeley, CA 94720. [‡]These authors contributed equally to this work.
[*]To whom correspondence should be addressed: mbfrancis@berkeley.edu

Supporting Information

Materials

Unless otherwise noted, all chemical reagents were purchased from Aldrich. Alexa Fluor® 488 C5-aminooxyacetamide, bis(triethylammonium) salt (AF488-ONH$_2$), Alexa Fluor® 647 C5-aminooxyacetamide, bis(triethylammonium) salt (AF647-ONH$_2$), N-(aminooxyacetyl)-N'-(D-biotinoyl) hydrazine, trifluoroacetic acid salt, and neutravidin-HRP were purchased from Invitrogen. M13KE and Anti-M13 p3 antibodies were purchased from New England Biolabs. O-(Methoxypoly(ethylene glycol))-hydroxylamine (PEG2k-ONH$_2$) was prepared as previously described.[1] Water used in biological procedures and chemical reactions was deionized using a NANOpure purification system (Barnstead, USA). All cell culture reagents were obtained from Gibco/Invitrogen Corp (Carlsbad, CA) unless otherwise noted.

Instrumentation

High performance liquid chromatography (HPLC). HPLC was performed on an Agilent 1100 Series HPLC System (Agilent Technologies, USA). Sample analysis for all HPLC experiments was achieved with an inline diode array detector (DAD) and an Agilent Zorbax 300 SB-CN column. 0.1% TFA/water (A) and 0.1% TFA/acetonitrile (B) were used as HPLC solvents. The following method was used: 35% B for the first 4 min, ramping to 70% B over 15 min, then to 95% B over the next 30 s, and a 5.5 min wash with 95% B.

Matrix assisted laser desorption-ionization time-of-flight mass spectrometry (MALDI-TOF MS). MALDI-TOF MS was performed on a Voyager-DE™ system (PerSeptiveBiosystems, USA) in the QB3/Chemistry Mass Spectrometry Facility. Sinipinic acid was used as the matrix.

Transmission electron microscopy (TEM). TEM images were obtained at the UC Berkeley Electron Microscope Lab (www.em-lab.berkeley.edu) using an FEI Tecnai 12 transmission electron microscope with a 100 kV accelerating voltage. Samples were prepared for TEM analysis by pipetting 8 μL of 0.1 nM fd solutions onto grids and allowing them to equilibrate for 3 min. The samples were wicked dry with filter paper, and the grids exposed to 8 μL of 10 mg/mL aqueous uranyl acetate solution for 90 s as a negative stain. The excess stain was removed by wicking, and the grid was allowed to dry in air.

Flow cytometry. A FACSCalibur flow cytometer (BD Biosciences, USA) equipped with 488 and 633 nm lasers were used for all flow cytometry measurements, usage courtesy of Prof. Carolyn Bertozzi (UC Berkeley).

Confocal microscopy. Images were acquired on a Zeiss 510 NLO Axiovert 200M Tsunami microscope equipped with 488 and 633 nm lasers, usage courtesy of Prof. Christopher Chang (UC Berkeley).

Zeta potential. Zeta potential measurements were obtained using a Malvern Instruments Zetasizer Nano ZS and DTS1060 cuvettes, usage courtesy of Prof. Jean M. J. Fréchet (UC Berkeley). Measurements were taken in water. Thirty measurements were taken per sample.

Calculation of phage concentration

phage/mL = ((absorbance at 269 nm – absorbance at 320 nm) / 6 x 10^6) / (number of single stranded DNA bases in the phage genome)[2]

Detailed Experimental Procedures

fd and M13KE phage growth and purification. fd phage displaying anti-EGFR, -HER2, and -BoNT scFvs were propagated in and reacted under identical conditions.[3–5] A tetracycline resistance gene was previously introduced into the fd phage genome to allow measurement of *E. coli* infectivity in colony forming units (cfu) using LB-agar plates containing 20 µg/mL tetracycline. A colony of *E. coli* TG1 cells infected with fd were inoculated into 2 mL of LB growth media containing 20 µg/mL tetracycline, incubated at 37 °C with 250 rpm shaking. After approximately 6 h, 1 mL culture was added to 1 L of 2xYT media containing 20 µg/mL tetracycline. The culture was incubated at 30 °C for approximately 13 h with 250 rpm shaking. Cells were removed via centrifugation at 6,000 rpm for 10-30 min at 4 °C. The supernatant was collected and the fd were precipitated for 1 h at 4 °C after thorough mixing with 0.15 volumes of 20% PEG8k/2.5M NaCl solution. The resulting suspension was centrifuged at 8,000 rpm for 20 min at 4 °C, and the recovered pellet was resuspended in 30 mL of 4 °C PBS. This solution of fd was centrifuged at 6,000 rpm for 10 min at 4 °C to remove additional cell debris. The supernatant was collected, and fd were precipitated for 40 min at 4 °C after thorough mixing with 0.15 volumes of a solution of 20% PEG8k and 2.5 M NaCl. The samples were then centrifuged at 9,000 rpm for 30 min to isolate the precipitated fd. The resulting pellet was resuspended in 5 mL of 4 °C PBS.

M13KE filamentous phage were used for western blotting experiments. Because M13KE lacks antibiotic resistance, it was grown from plaques rather than colonies. It was grown in media lacking antibiotics at 37 ºC and its purification was identical to that used for fd.

Transamination. fd and M13KE were transaminated using 100 mM pyridoxal-5'-phosphate (PLP) in 100 mM phosphate buffer, pH 6.5, for 13 h at rt. Concentrations of 75-128 nM fd were used in these experiments, typically at total volumes of 5-20 mL. Due to the large excess of PLP used, fd concentration was not found to be critical for successful transamination. As an example reaction: 4.7 mL of water was added to 3.3 mL of 128 nM anti-EGFR fd, followed by 1 mL of 250 mM phosphate buffer at pH 6.5, and 1 mL of 1 M PLP in 125 mM phosphate buffer, pH 6.5. The transamination was allowed to proceed for approximately 13 h, at which point the excess PLP was removed by a series of precipitations and resuspensions in PBS. After thorough mixing with 0.15 volumes of a 20% PEG8k/2.5 M NaCl solution, the fd were precipitated for 1 h at 4 °C. The fd were then isolated by centrifugation at 9,000 rpm for 30 min. The fd pellet was resuspended in 30 mL of PBS, and then the precipitation, centrifugation, and

S2

resuspension cycle was repeated two additional times. The final pellet was resuspended in PBS to yield a final volume of approximately 2 mL. To prepare the PLP solution used in these reactions, a 2 M solution of PLP in 250 mM phosphate buffer (pH 6.5) was made. The pH was adjusted to 6.5 with 3 M NaOH, and the solution was diluted with 250 mM phosphate buffer, pH 6.5 to give a 1 M PLP solution. The PLP solution must be freshly made before use.

Reaction with 2-(aminooxy)acetic acid. 24 nM transaminated fd was reacted with 5 mM 2-(aminooxy)acetic acid in 100 mM anilinium acetate, pH 4.7, for 21 h at rt. For M13KE, 25 nM transaminated M13KE was reacted with 7 mM 2-(aminooxy)acetic acid in 100 mM phosphate buffer, pH 4 with 1 mM aniline for 21 h at rt. Both reactions conditions yield approximately equivalent percentages of oxime product (Supporting Information Figure S1 and S3).

M13KE reaction with biotin and western blotting. M13KE filamentous phage were used for biotin labeling as an fd surrogate because fd could not be sufficiently concentrated to observe all minor coat proteins by western blot. M13KE is a one amino acid variant of fd, and is shorter because its genome has not been enlarged by genetic engineering. This decrease in length enables higher minor coat protein concentrations to be obtained.[2] The final reaction concentrations were: 296 nM M13KE, 10 mM phosphate buffer (pH 6.2), 10 mM aniline, and 16 mM biotin-ONH_2. After 15 h at rt, the reaction was quenched by adding DL-glyceraldehyde to a final concentration of 33.3 μM, followed by SDS-PAGE. A 1:10,000 dilution of anti-p3 antibodies and a 1:2,000 dilution of Neutravidin-HRP were used for blotting. A Genscript 1-hour western kit was used for detection.

Conjugation of fluorophores to ketone-modified fd phage. A sample of ketone-labeled fd phage prepared as described above was exposed to the appropriate alkoxyamine and an aniline catalyst[6] in an Eppendorf tube. The final reaction concentrations were: 185 nM fd, 20 mM phosphate buffer pH 6.2, aniline (10 mM for AF-488 or 100 mM for AF-647, as a catalyst for the oxime formation), and 1 mM fluorophore. Total reaction volumes were typically <100 μL. The reaction was quenched by fd precipitation and solution removal after 45 min at rt, resulting in 2% p8 labeling with the fluorophore. For higher levels of modification, the reactions were allowed to proceed for up to 18 h. Levels of modification were calculated using the extinction coefficients of the fluorophores (AF488: 71,000 M^{-1} cm^{-1}, AF647: 237,000 M^{-1} cm^{-1} according to Molecular Probes/Invitrogen) to determine the fluorophore concentration. After the fluorophore contribution to the 269 and 320 nm absorbance has been subtracted from the total 269 and 320 nm absorbance, the fd concentration can be calculated. Excess fluorophore was removed in an analogous fashion to the removal of excess PLP.

Conjugation of PEG2k to ketone-modified fd phage. Fluorophore labeled fd were reacted with PEG2k-ONH_2 for varying lengths of time. The conditions for the PEG2k-ONH_2 reaction were: 37 nM phage, 20 mM PEG2k-ONH_2, 20 mM phosphate buffer pH 6.2, and 10 mM aniline. After 1.5, 4, and 22 h at rt, aliquots from the reaction mixture were washed over an Illustra Nap-5 gel filtration column (GE Healthcare). If desired, DL-glyceraldehyde can also be used to quench the reaction before passing it over an Illustra Nap-5 gel filtration column; however, this quench was not used for the samples described in this report. The extent of PEG2k labeling was quantified using reverse phase HPLC. The typical p8 coat protein elution time was 10-13 min.

Zeta potential measurement. Zeta potential measurements were performed using a Zetasizer Nano-DS and DTS1060 cuvettes. fd labeled with PEG2k, but not with fluorophore, were used. Following the PEG conjugation reaction, the fd were eluted from NAP-5 columns in water to improve the reproducibility of the zeta-potential measurements.

Cell culture. Immortalized human breast cancer cells were maintained according to ATCC guidelines. SUM52PE cells were from the Tissue Culture Facility, Department of Molecular & Cell Biology, UC Berkeley, and were grow in Ham's F-12 media supplemented with 5% FBS, 5 µg/mL insulin, 1 µg/mL hydrocortisone, and 10 mM HEPES (pH 7.4). MCF-7 clone 18 cells were from the Preclinical Therapeutics Core Facility, UCSF. All cells were grown at 37 °C in 5% CO_2.

Cell microscopy. Cells were washed with PBS, trypsinized, and trypsin was quenched with growth media. Cells were centrifuged at 125 rcf for 5 min, and resuspended in growth media. Following counting via hemocytometer, the cells were centrifuged again, and resuspended in normal growth media at a concentration of 25,000 cells/mL. 2 mL was added to each 35 mm glass bottom dish (MatTek Corp.). For MCF-7 clone 18/MDA-MB-231 co-cultures, 1 mL (25,000 cells/mL) of each cell line was added to a centrifuge tube and mixed by pipetting prior to plating in dishes together. Cells were allowed to grow at 37 °C with 5% CO_2 for 72-96 h. All media was removed from the dishes, and cells were washed once with 1 mL PBS. 150 µL of 0.8 nM fd in flow cytometry buffer (FCB, see below) was added to each well of the plate, and the dishes were incubated at 37 °C with 5% CO_2. After 1 h, 1 mL of PBS was added to wash the cells gently, and was then removed. Two more washes with 1 mL of PBS were performed, and then 1 mL of phenol red-free media with 10% FBS was added to the cells. DAPI was added to 1 µM prior to imaging.

Flow cytometry. Following the harvesting and counting of cells as above, cells were resuspended in flow cytometry buffer (FCB; 1% FBS in DPBS). The cells were aliquotted into Eppendorf tubes at 100 µL (500,000 cells) per tube and kept on ice. 100 µL of 0.8 nM fd in FCB was added and incubated at 4 ºC. After 1 h, each sample was diluted to 1 mL with FCB, and the tubes were centrifuged at 2,000 rpm for 5 min. The supernatant was removed, and the cells were resuspended in 1 mL of FCB, followed by centrifugation, and removal of the supernatant. The cells were finally resuspended in 200 µL of FCB. Data were analyzed using FlowJo analysis software (Tree Star Inc.). Gating was performed by applying the autogating tool in FlowJo onto the major population of cells in the FSC x SSC (forward versus side scatter plots) of untreated samples; additional (agent treated) samples were subject to the same gating as the untreated populations for that respective cell line.

Supporting Information References
[1] Schlick, T. L.; Ding, Z.; Kovacs, E. W.; Francis, M. B. Dual-Surface Modification of the Tobacco Mosaic Virus. *J. Am. Chem. Soc.* **2005**, *127*, 3718-3723.
[2] Barbas, C. F.; Burton, D. R.; Scott, J. K.; Silverman, G. J. *Phage Display: A Laboratory Manual*; Cold Spring Harbor Laboratory Press: Cold Spring Harbor, New York, **2001**.
[3] Zhou, Y.; Drummond, D. C.; Zou, H.; Hayes, M. E.; Adams, G. P.; Kirpotin, D. B.; Marks, J. D. Impact of Single-Chain Fv Antibody Fragment Affinity on Nanoparticle Targeting of Epidermal Growth Factor Receptor-Expressing Tumor Cells. *J. Mol. Biol.* **2007**, *371*, 934-947.
[4] Amersdorfer, P.; Wong, C.; Smith, T.; Chen, S.; Deshpande, S.; Sheridan, R.; Marks, J. D. Genetic and Immunological Comparison of Anti-Botulinum Type A Antibodies from Immune and Non-Immune Human Phage Libraries. *Vaccine* **2002**, *20*, 1640-1648.

S4

[5] O'Connell, D.; Becerril, B.; Roy-Burman, A.; Daws, M.; Marks, J. D. Phage Versus Phagemid Libraries for Generation of Human Monoclonal Antibodies. *J. Mol. Biol.* **2002**, *321*, 49-56.

[6] Dirksen, A.; Hackeng, T. M.; Dawson, P. E. Nucleophilic Catalysis of Oxime Ligation. *Angew. Chem., Int. Ed.* **2006**, *45*, 7581-7584.
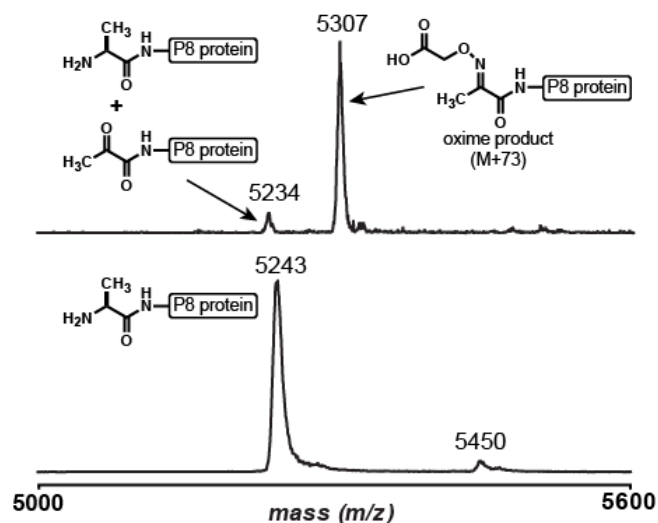
Figure S1. MALDI-TOF spectrum of transaminated fd (top) and non-transaminated fd (bottom) following reaction with 2-(aminooxy)acetic acid. The expected molecular weight of p8 is 5240 Da. The observed 5234 *m/z* peak (top) and the 5243 m/z peak (bottom) correspond to the transaminated and/or unmodified p8 proteins. The peak at 5307 m/z (top) corresponds to the oxime product (expected mass increase: 73 m/z, observed 73 *m/z*).

S6
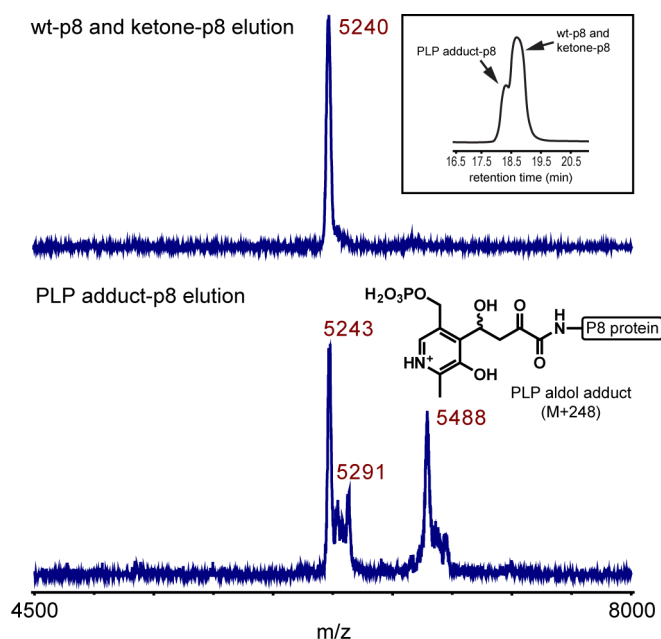
Figure S2

Figure S2. Characterization of modified M13KE phage p8 using MALDI-TOF MS after M13KE transamination and separation of p8 modifications via reversed phase HPLC. (Inset) HPLC chromatogram of modified M13KE. (Top) MALDI-TOF spectrum corresponding to the major peak of the p8 elution (see Figure S13, top spectrum for the analogous elution profile of fd). The expected molecular weight of wt-p8 is 5239 Da and overlaps with that of the expected ketone-p8 mass of 5238 Da. (Bottom) MALDI-TOF spectrum of the shoulder-peak, which elutes slightly before the main peak, corresponding to the PLP adduct-P8; some of the major elution peak bleeds into this peak, explaining the 5243 Da signature. The 5291 peak is of unknown origin. The observed mass difference between the two major MALDI peaks is 245 Da, which is presumably an aldol addition of the ketone group to the PLP aldehyde (expected change: 248 Da).

Figure S3
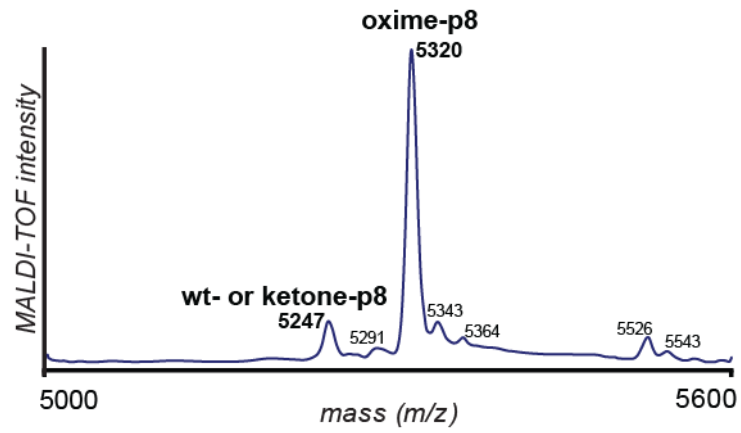
Figure S3. Characterization of modified M13KE phage using MALDI-TOF MS. The spectrum shows p8 oxime formation following reaction with 2-(aminooxy)acetic acid (expected mass increase: 73 m/z, observed: 73 m/z). The smaller peaks cannot be attributed to any coat protein and are of unknown origin.
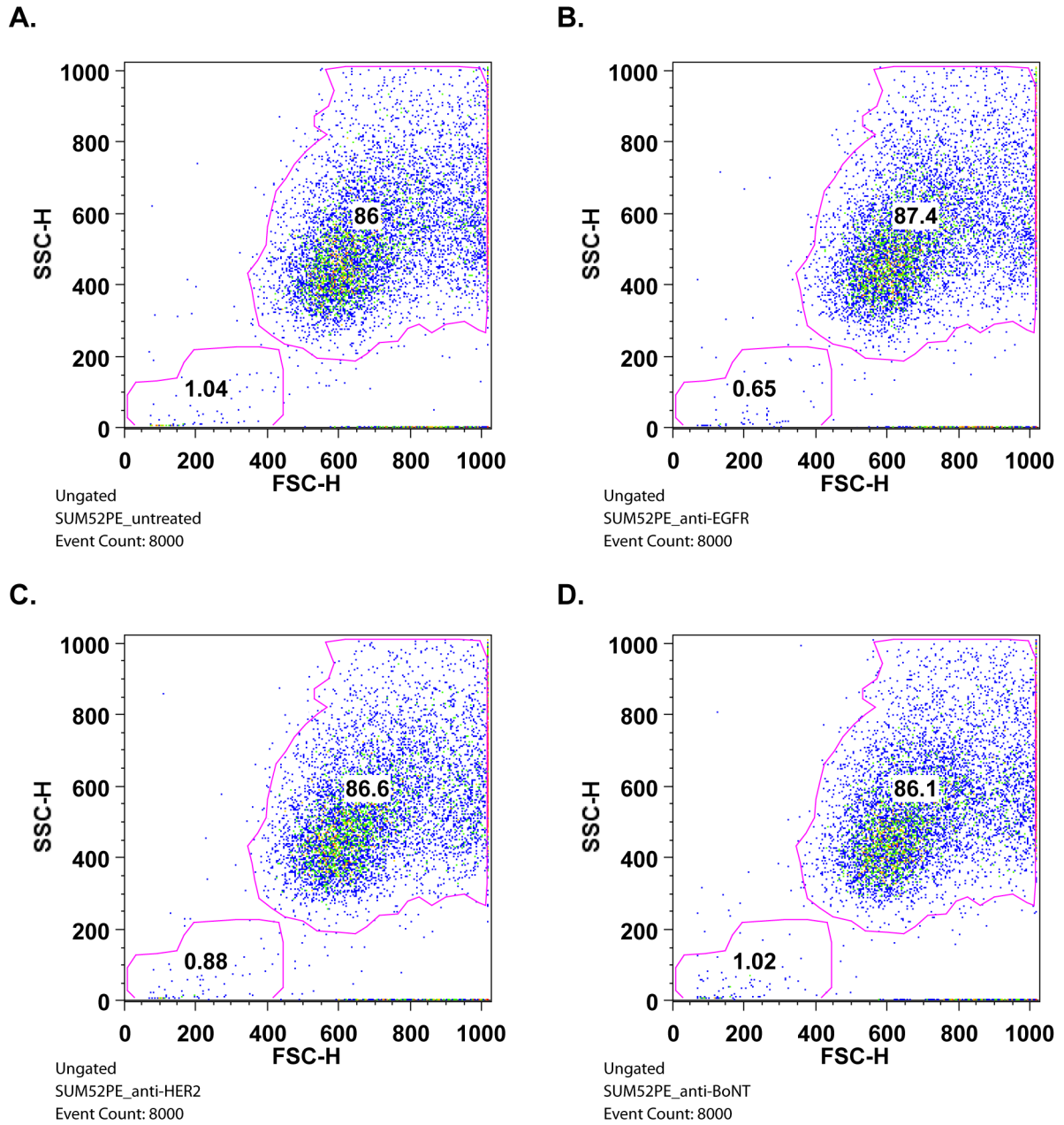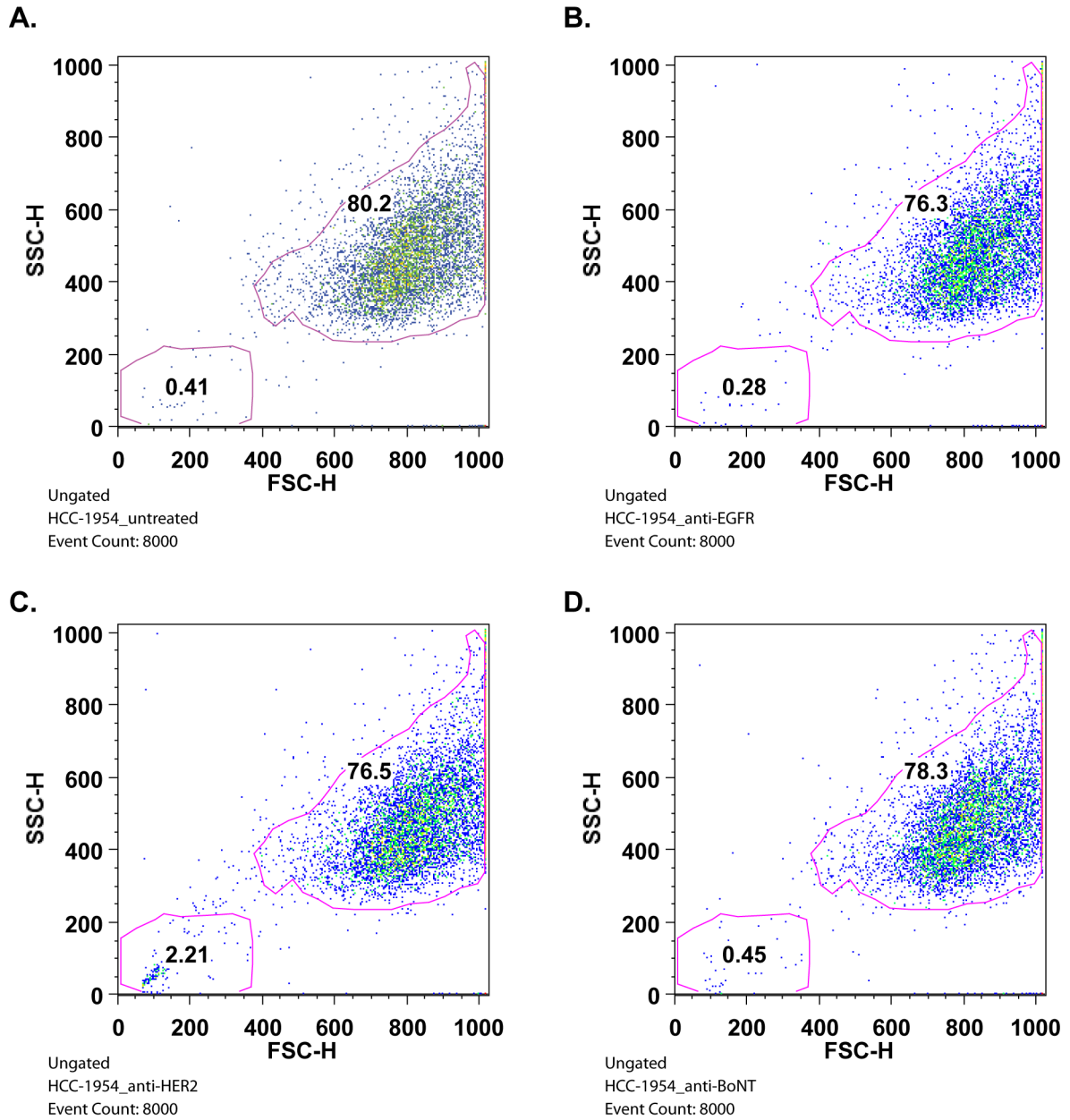
Figure S4. Forward and side scatter plots for flow cytometry with SUM52PE cells. Plots are shown for (**A**) untreated, (**B**) anti-EGFR phage treated, (**C**) anti-HER2 phage treated, and (**D**) anti-BoNT treated cells. The gating of the majority population was used for histogram generation (Figure 3a) as indicated by the pink outline; the gating of the minority population reflects dead or dying cells. Number inside of the plot reflects percentage of cells within each gate.
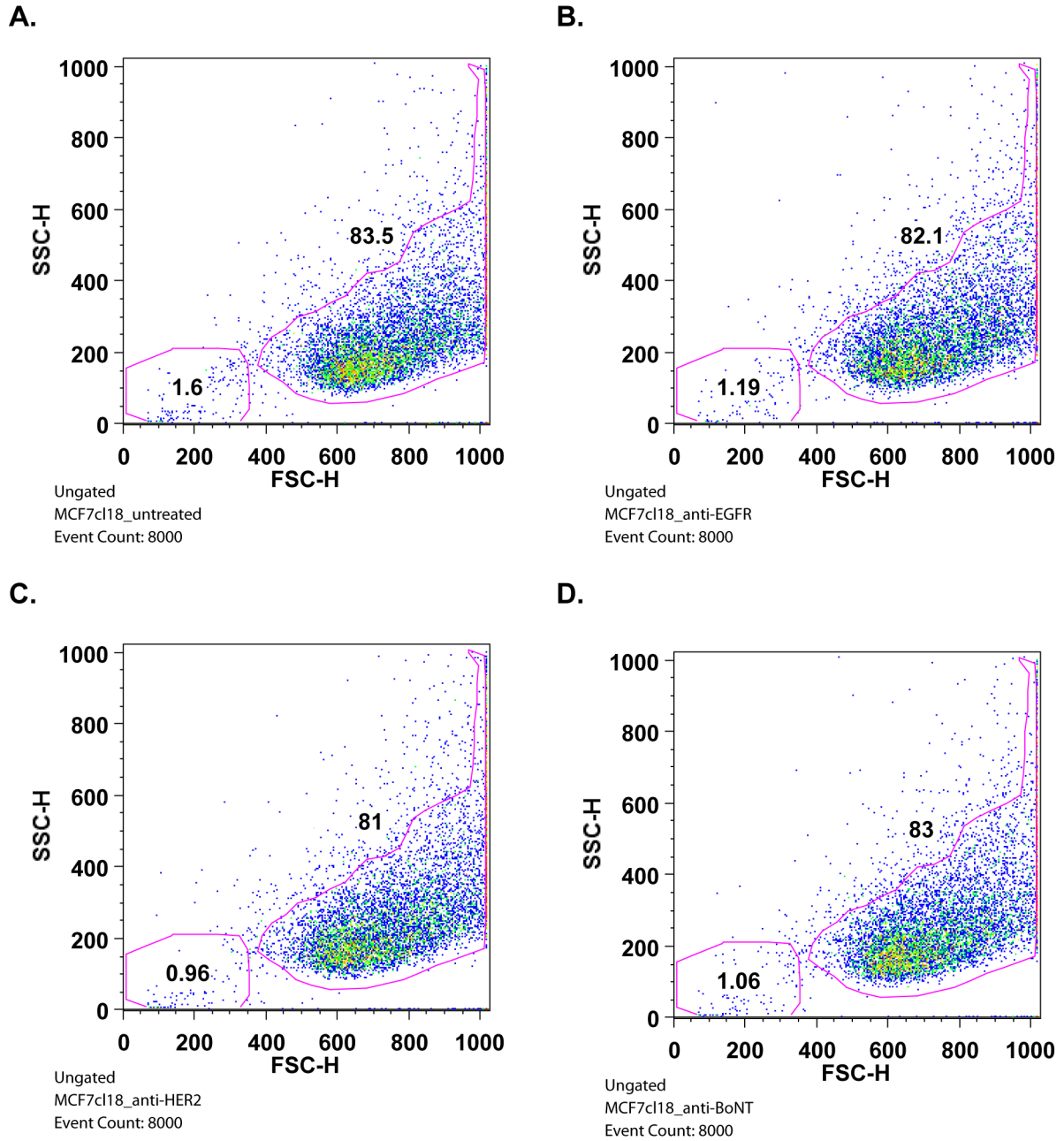
Figure S5. Forward and side scatter plots for flow cytometry with MCF-7 clone 18 cells. Plots are shown for (**A**) untreated, (**B**) anti-EGFR phage treated, (**C**) anti-HER2 phage treated, and (**D**) anti-BoNT treated cells. The gating of the majority population was used for histogram generation (Figure 3a) as indicated by the pink outline; the gating of the minority population reflects dead or dying cells. Number inside of the plot reflects percentage of cells within each gate.
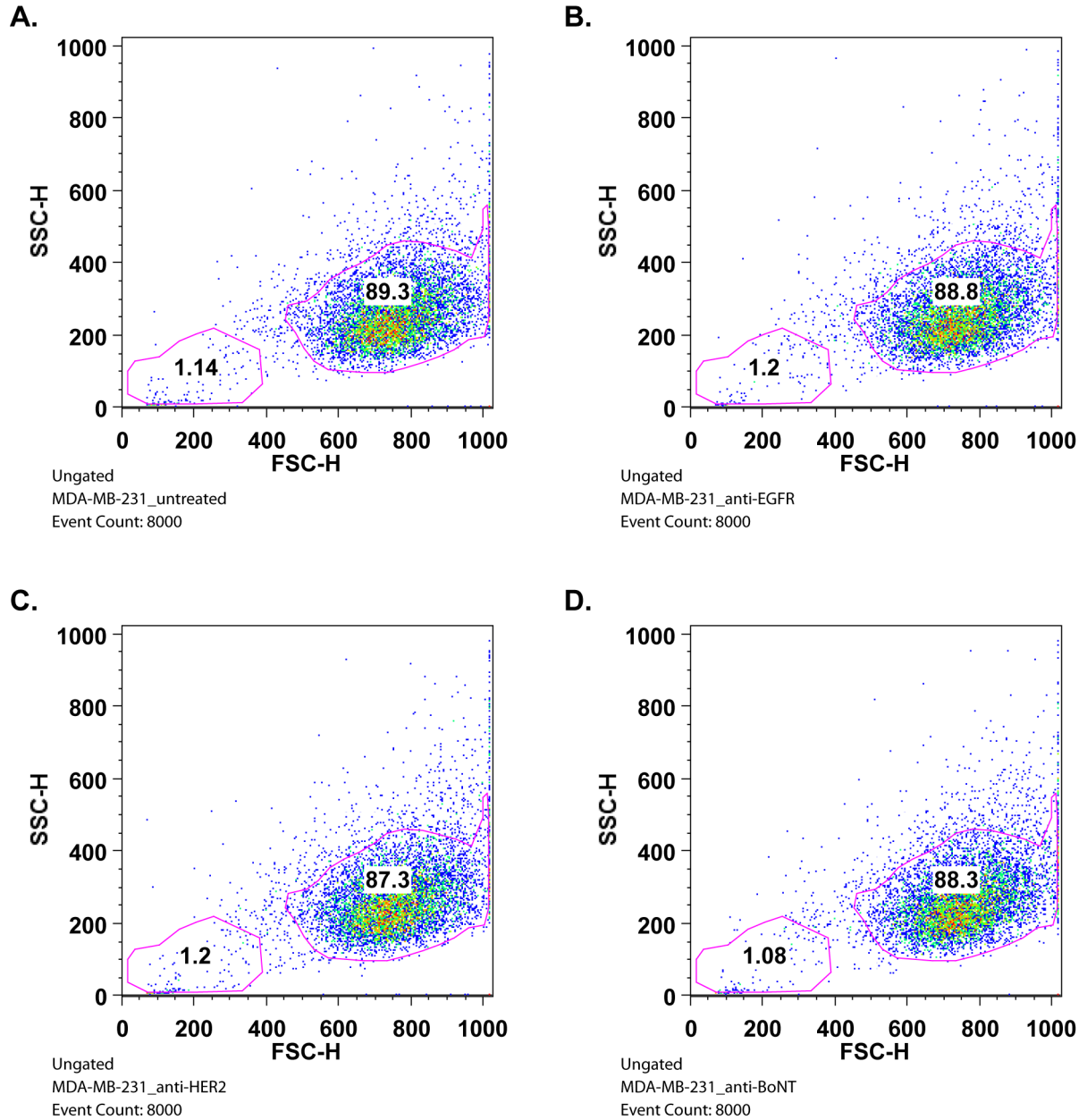
Figure S6. Forward and side scatter plots for flow cytometry with MDA-MB-231 cells. Plots are shown for (**A**) untreated, (**B**) anti-EGFR phage treated, (**C**) anti-HER2 phage treated, and (**D**) anti-BoNT treated cells. The gating of the majority population was used for histogram generation (Figure 3a) as indicated by the pink outline; the gating of the minority population reflects dead or dying cells. Number inside of the plot reflects percentage of cells within each gate.

Figure S7. Forward and side scatter plots for flow cytometry with HCC1954 cells. Plots are shown for (**A**) untreated, (**B**) anti-EGFR phage treated, (**C**) anti-HER2 phage treated, and (**D**) anti-BoNT treated cells. The gating of the majority population was used for histogram generation (Figure 3a) as indicated by the pink outline; the gating of the minority population reflects dead or dying cells. Number inside of the plot reflects percentage of cells within each gate.

A.

B.
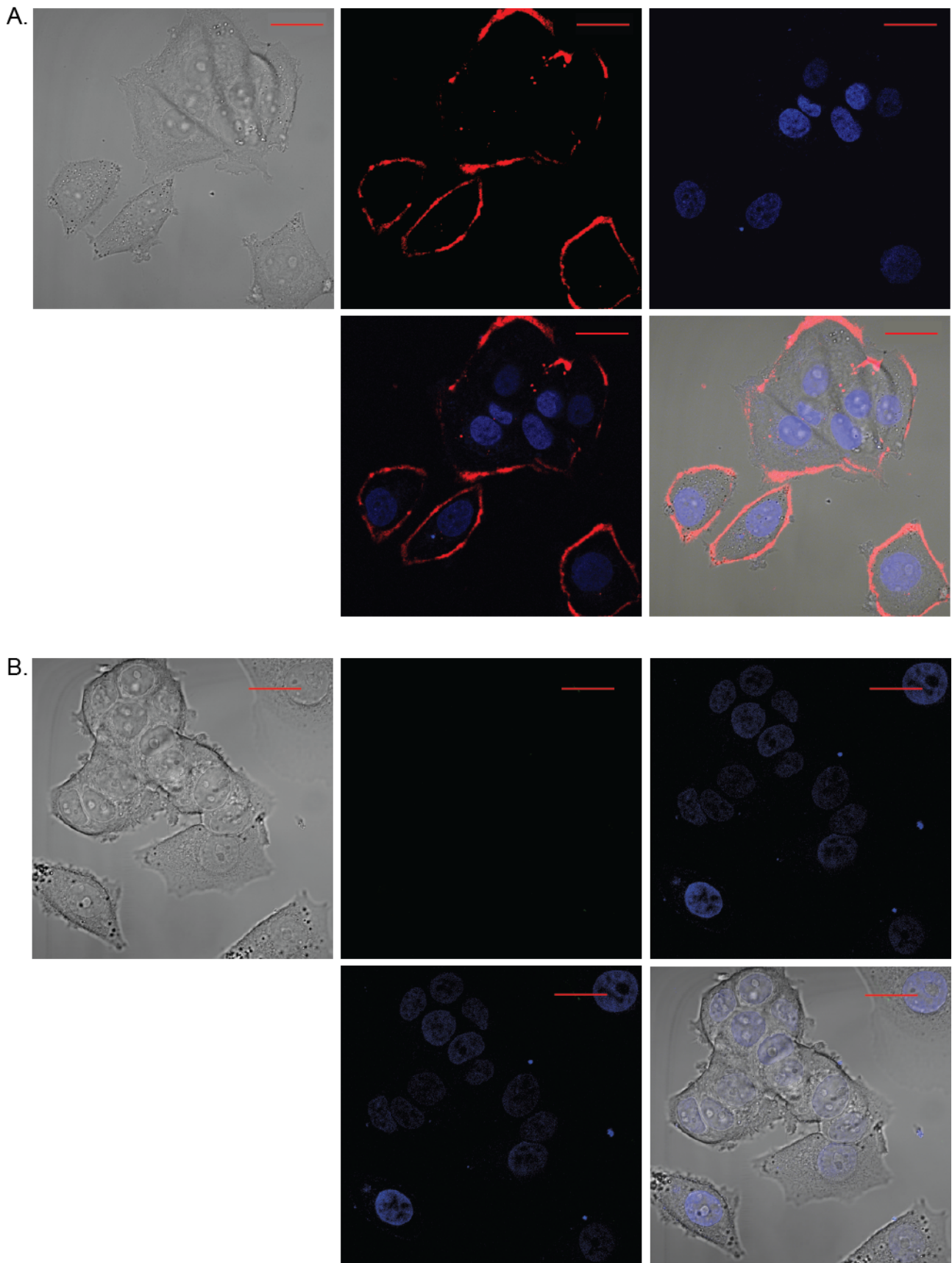
Figure S8. Live cell confocal microscopy images of MCF-7 clone 18 cells treated with anti-HER2 (**A**) and anti-EGFR (**B**) fd. Fd were added at 0.8 nM in 150 μL of PBS. Scale bars indicate 20 μm. Fluorescence is as follows: DAPI (blue), anti-HER2

(red), anti-EGFR (green). Top row (L to R): bright field image, red (**A**) or green (**B**) channel only, blue channel only; bottom row (L to R): all fluorescence channels, merge.
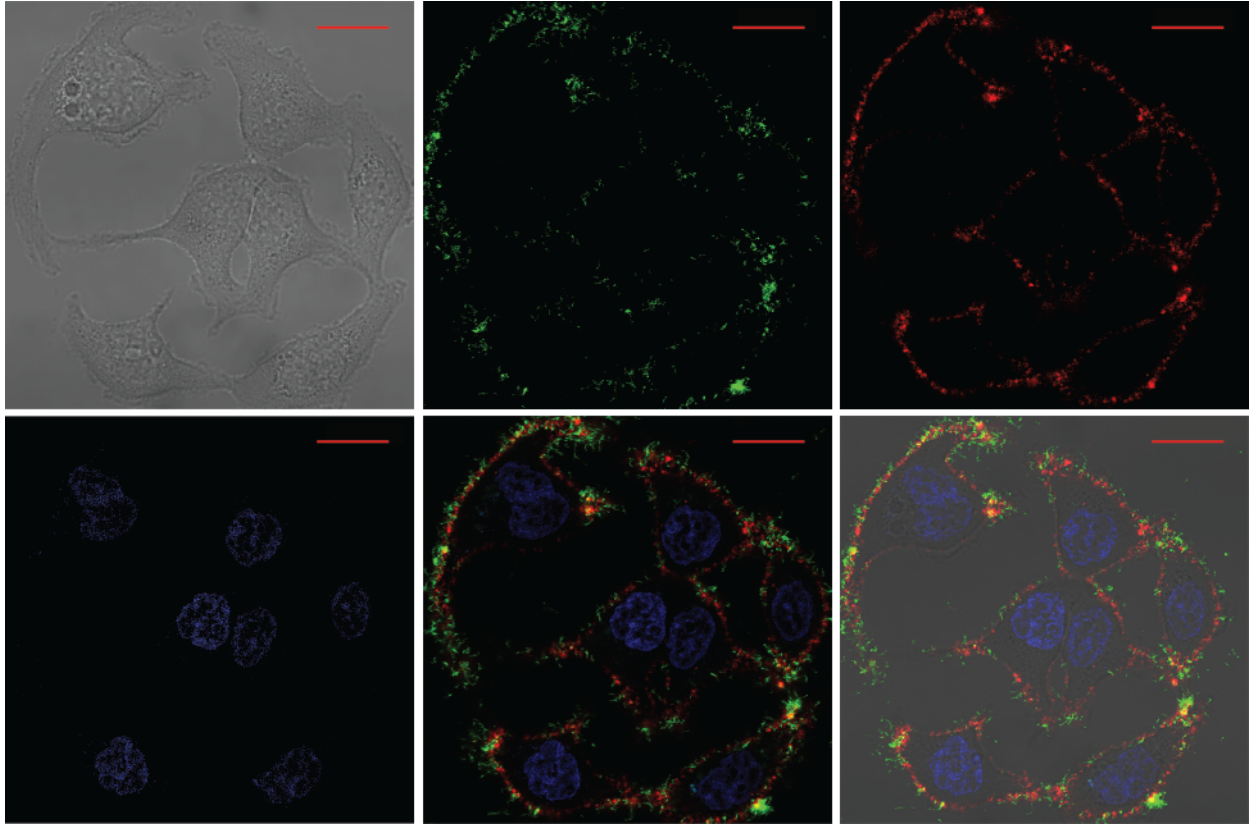
S14
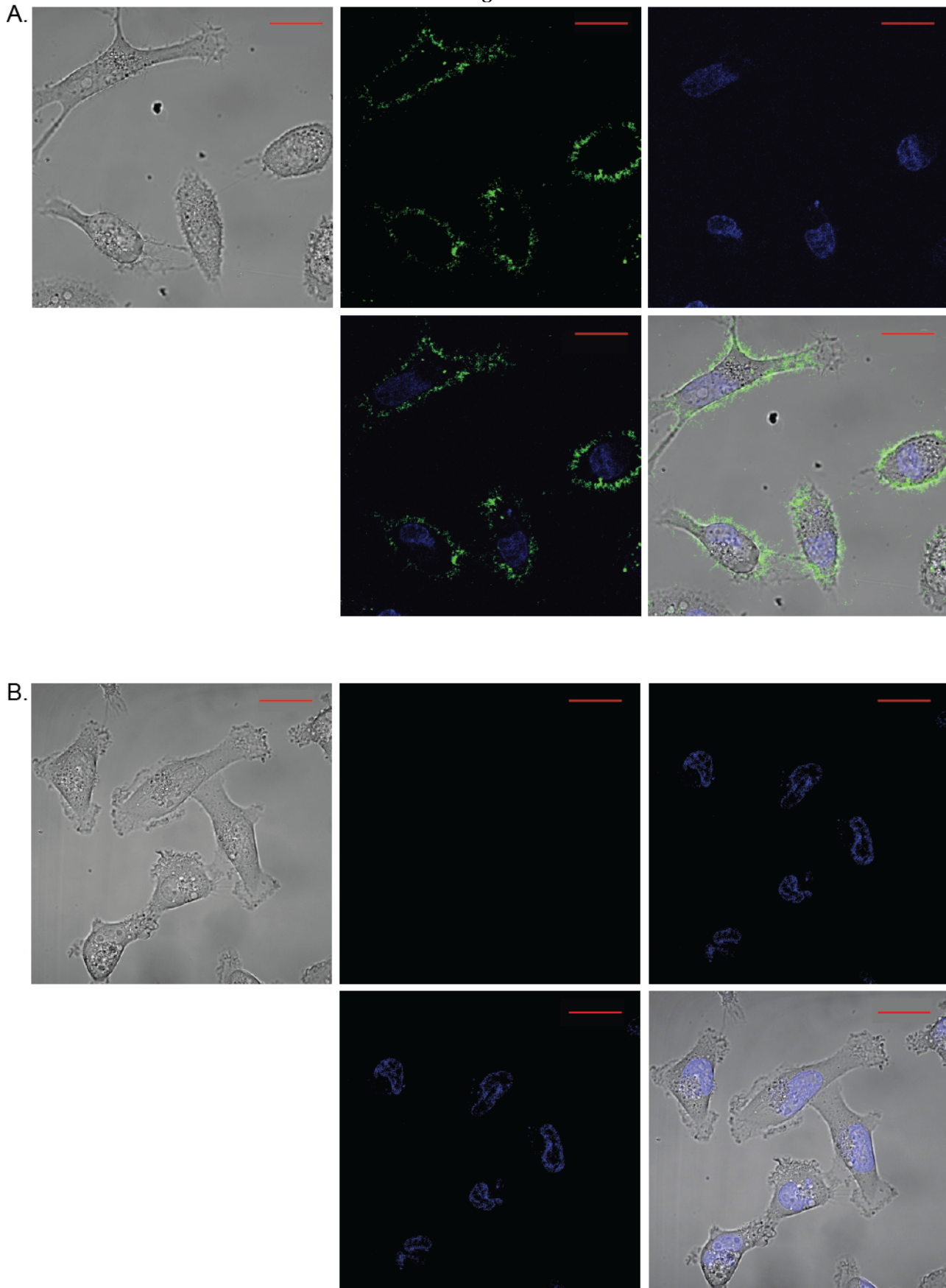
Figure S9. Live cell confocal microscopy images of MDA-MB-231 cells treated with anti-EGFR (**A**) and anti-HER2 (**B**) fd. Fd were added at 0.8 nM in 150 μL of PBS. Scale bars indicate 20 μm. Fluorescence is as follows: DAPI (blue), anti-HER2 (red), anti-EGFR (green). Top row (L to R): bright field image, green (**A**) or red (**B**) channel only, blue channel only; bottom row (L to R): all fluorescence channels, merge.
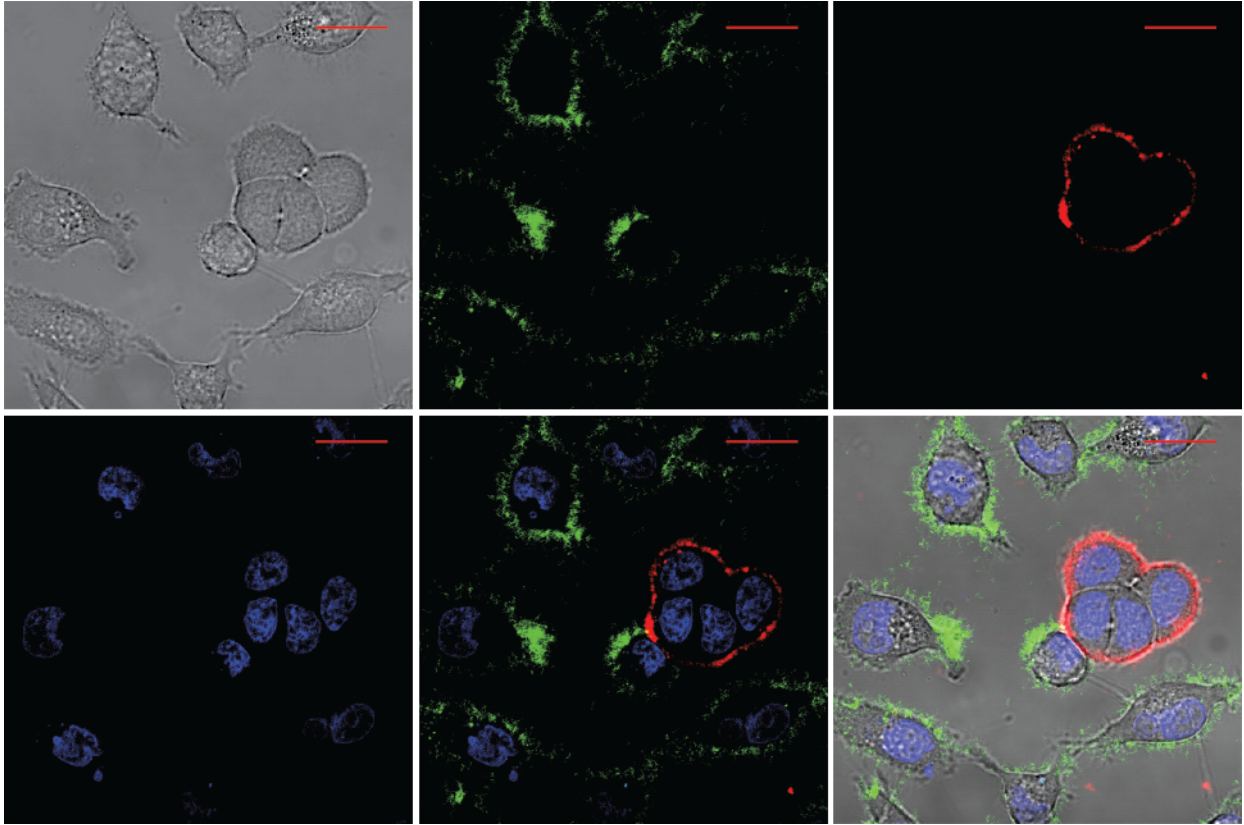
Figure S10. Live cell confocal microscopy images of MDA-MB-231 and MCF7 clone 18 cells treated with anti-HER2 and anti-EGFR fd. Fd were added at 0.8 nM in 150 μL of PBS. Scale bars indicate 20 μm. Fluorescence is as follows: DAPI (blue), anti-HER2 (red), anti-EGFR (green). Top row (L to R): bright field image, green channel only, red channel only; bottom row (L to R): blue channel only, all fluorescence channels, merge.

Figure S11. Live cell confocal microscopy images of HCC1954 cells treated with anti-HER2 and anti-EGFR phage. Phage were added at 0.8 nM in 150 μL of PBS. Scale bars indicate 20 μm. Fluorescence is as follows: DAPI (blue), anti-HER2 (red), anti-EGFR (green). Top row (L to R): bright field image, green channel only, red channel only; bottom row (L to R): blue channel only, all fluorescence channels, merge.

A.

B.

Figure S12. Live cell confocal microscopy images of SUM52PE cells treated with anti-HER2 (**A**) and anti-EGFR phage (**B**). Phage were added at 0.8 nM in 150 μL of PBS. Scale bars indicate 20 μm. Fluorescence is as follows: anti-HER2 (red), anti-EGFR (green). (L to R): bright field image, red channel only (**A**) or green channel only (**B**), merge. Due to cellular toxicity, nuclear staining was not used with these cells.
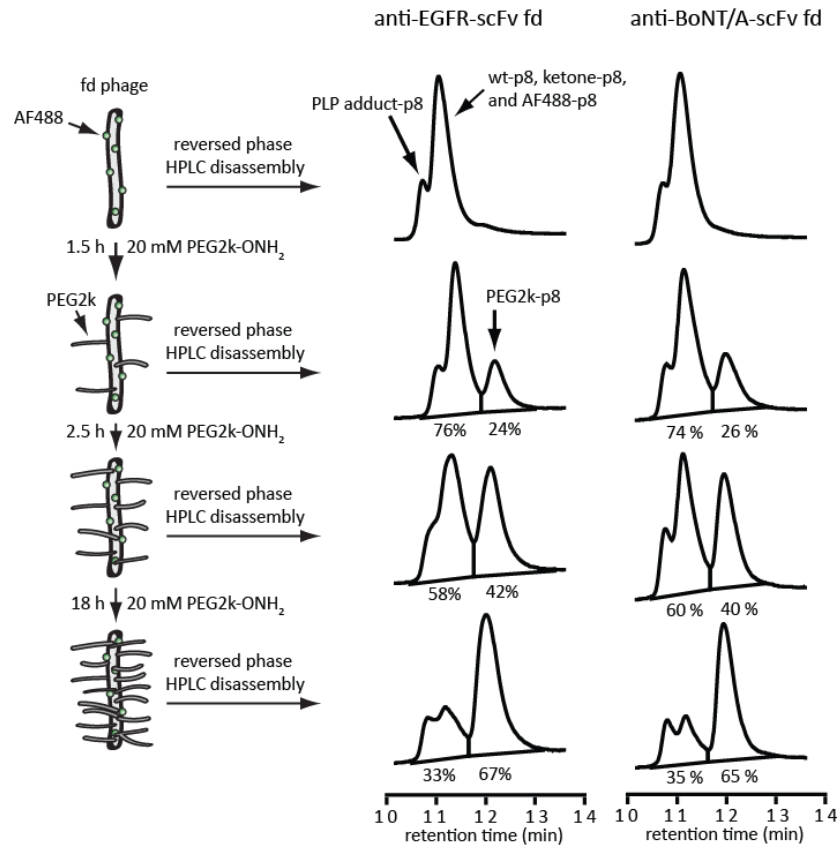
Figure S13. PEG2k modification of fd**.** After transamination using PLP and modification with AF488-ONH$_2$, the fd were reacted with 20 mM PEG2k-ONH$_2$ for 1.5, 4, and 22 h. During reversed phase chromatography, the fd disassembled into coat proteins and DNA. The absorbance at 280 nm is shown; p8 was the only coat protein observed. The first peak to elute corresponds to the PLP adduct of p8 (see Figure S2). The second peak is composed of wt-p8, ketone-p8, and AF488-p8 (absorbance at 488 nm is observed), and the last peak to elute (PEG-treated samples only) is PEG2k-p8.
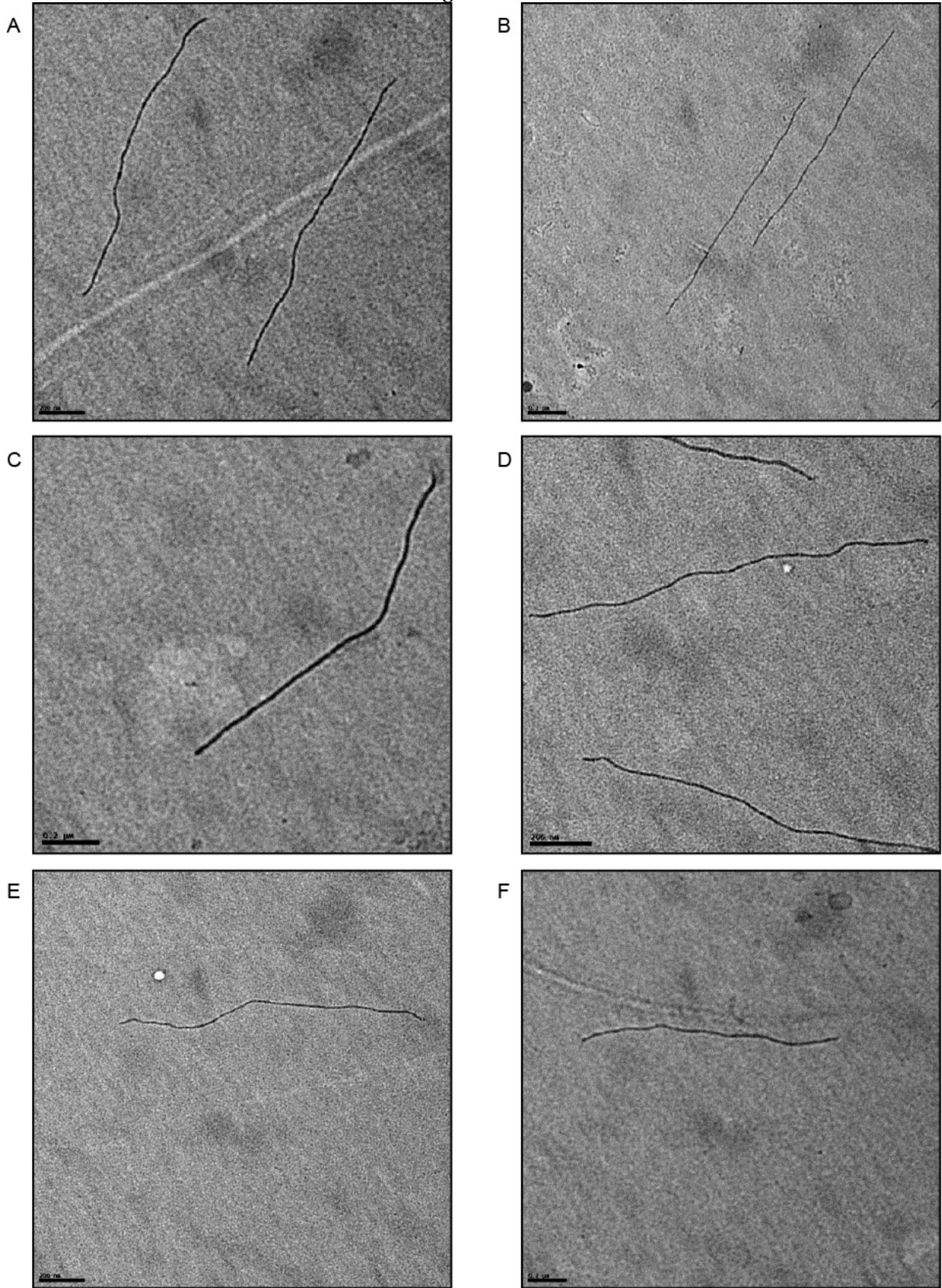
Figure S14. Transmission electron microscope (TEM) images of fd bearing anti-EGFR-scFv molecules**. (A)** Wt-fd. (**B**) Fd following PLP-mediated transamination. (**C**) Fd with 2% of the p8 proteins fluorescently labeled with AF488-ONH$_2$, **(D)** 2% AF488 and 24% PEG2k, (**E**) 2% AF488 and 42% PEG2k, and (**F**) 2% AF488 and 67% PEG2k. All scale bars represent 200 nm.
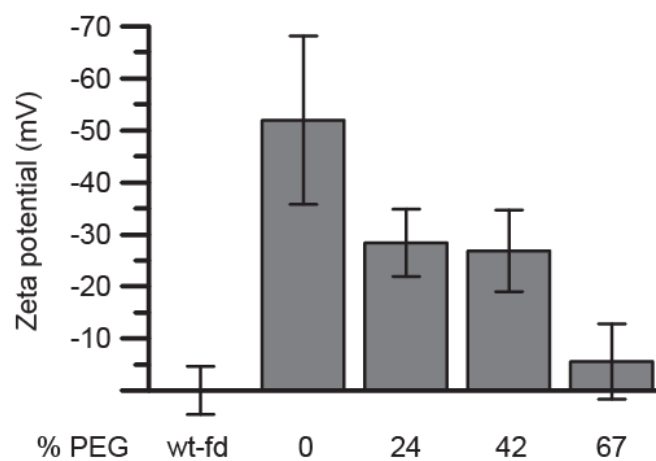
Figure S15. Zeta potential measurements of anti-EGFR fd as a function of the percent of p8 proteins labeled with PEG2k. These fd phage have not been modified with AF488.
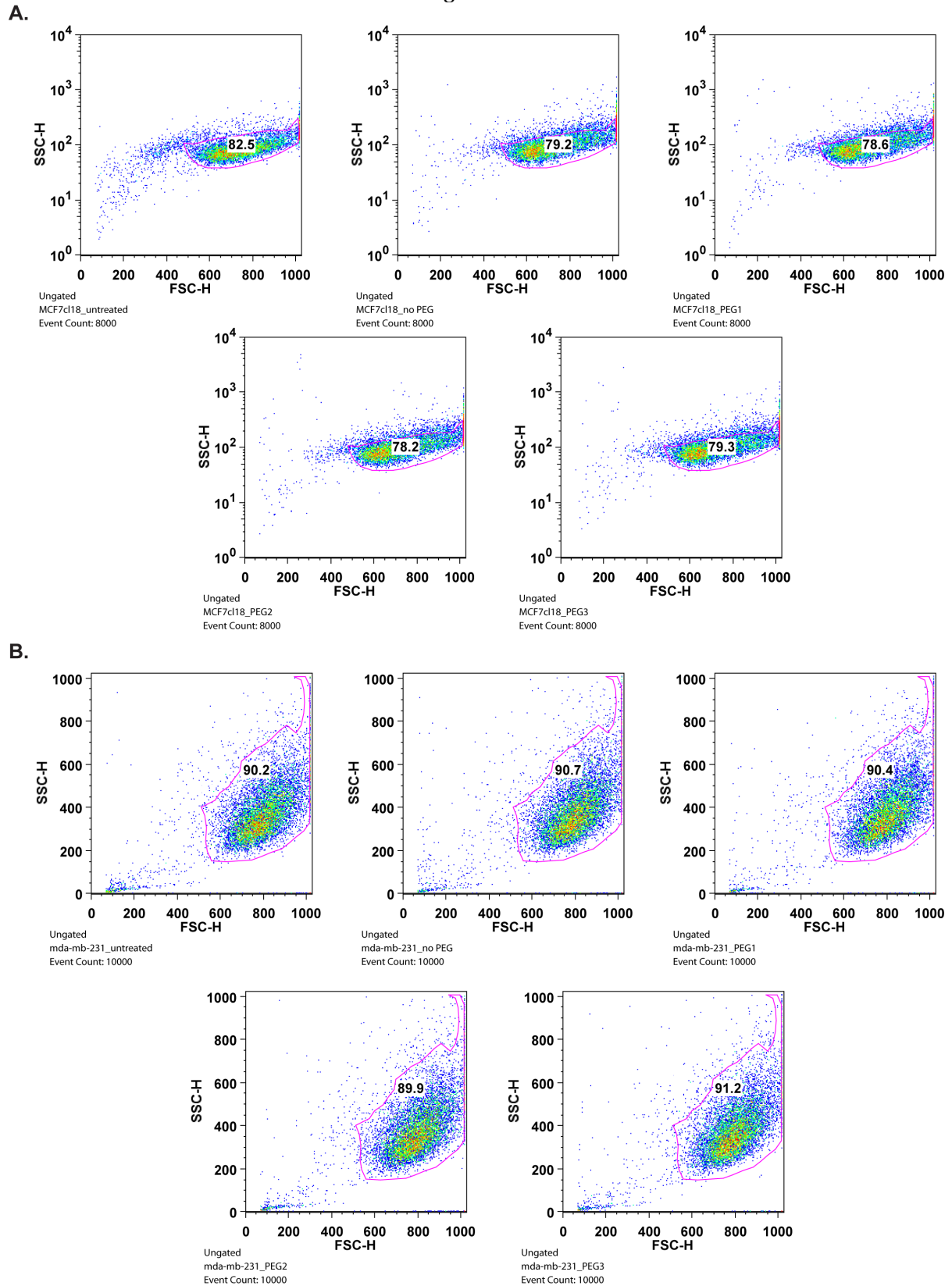
Figure S16. Forward and side scatter plots for flow cytometry with MCF-7 clone 18 (**A**) and MDA-MB-231 (**B**) cells. Plots are shown for untreated, no-PEG (0% modified), PEG1 (15% modified), PEG2 (48% modified), and PEG3 (74% modified) anti-EGFR treated cells. The gating of the majority population was used for histogram generation (Figure 4 in main text) as indicated by the pink outline. The number inside of the plot reflects percentage of cells within each gate.
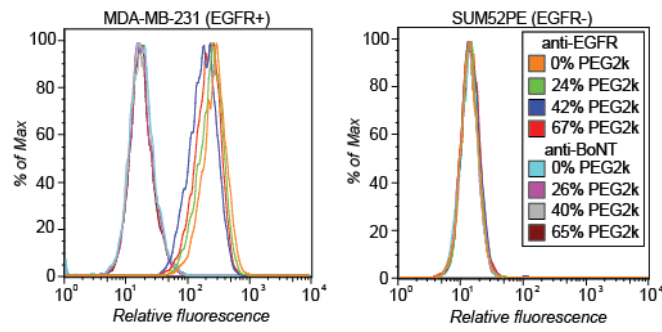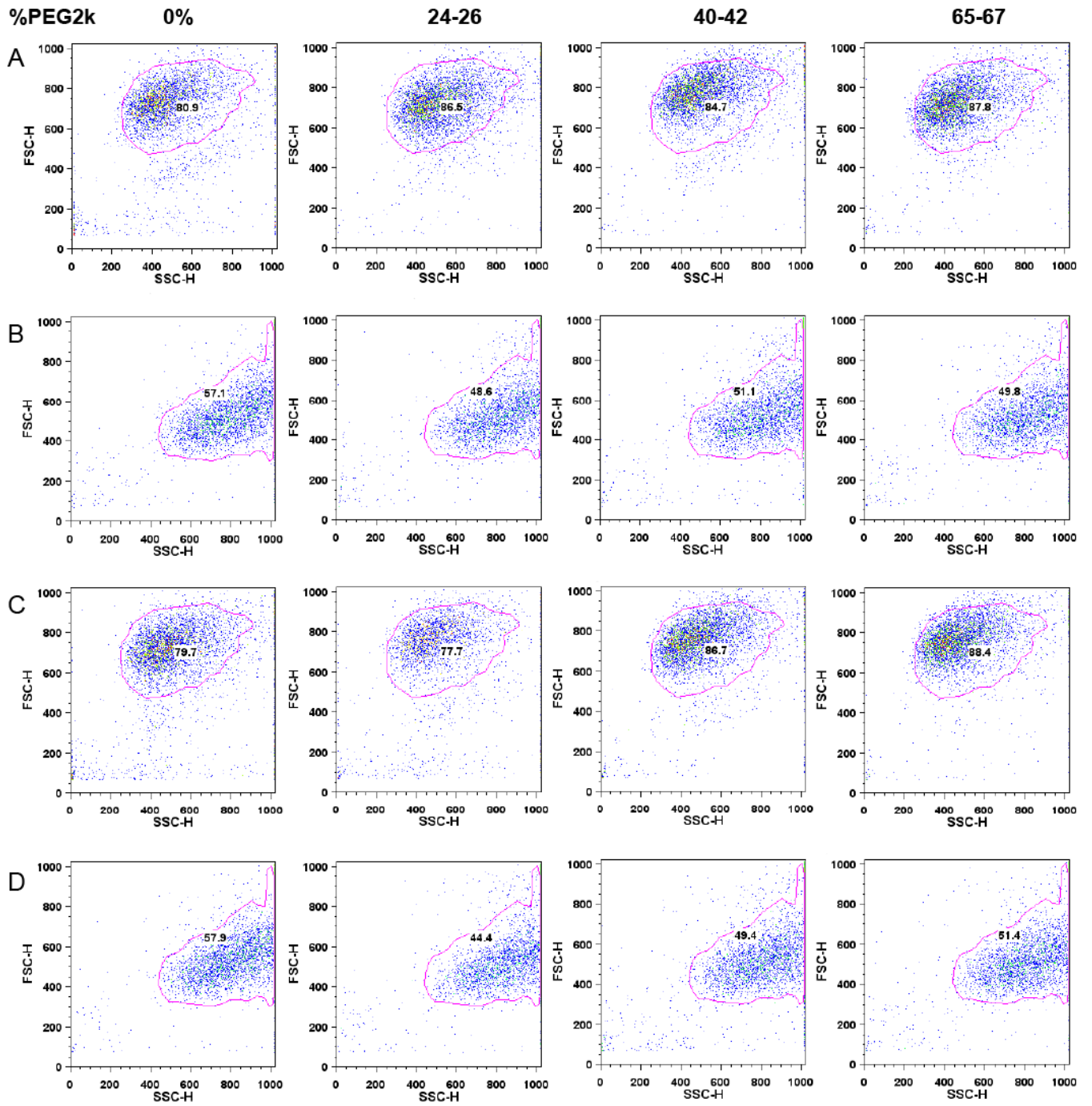
Figure S17. Histograms of MDA-MB-231 (left) and SUM52PE (right) cell-binding by anti-EGFR and anti-BoNT fd with various percentages of p8 proteins labeled with PEG2k.

Figure S18. Forward and side scatter plots for flow cytometry with PEG-modified phage. Columns (L to R) indicate p8 proteins modified with various percentages of PEG2k. Plots are shown for (**A**) anti-EGFR fd treated MDA-MB-231 cells, (**B**) anti-EGFR fd treated SUM52PE cells, (**C**) anti-BoNT fd treated MDA-MB-231 cells, and (**D**) anti-BoNT fd treated SUM52PE cells. Gating used for histogram generation (Figure S17) is indicated by the pink outline. The number inside of the plot reflects percentage of cells within each gate.